Supplementary Information

Carbazole-Containing Difluoroboron β-Diketonate dyes: two-photon excited fluorescence in solution and grinding-induced blue-shifted emission in solid state

Peng-Zhong Chen,[a] Jian-Xin Wang,[a] Li-Ya Niu,*[a] Yu-Zhe Chen[b] and Qing-Zheng Yang*[a]

[a] Key Laboratory of Radiopharmaceuticals, Ministry of Education, College of Chemistry, Beijing Normal University, Beijing 100875, China. *E-mail*: niuly@bnu.edu.cn, qzyang@bnu.edu.cn

[b] Key Laboratory of Photochemical Conversion and Optoelectronic Materials, Technical Institute of Physics and Chemistry, Chinese Academy of Sciences, Beijing 100190, China.

Methods and Materials 2

Scheme S1. The synthetic routes of complexes **1**-**4**. 3

Fig. S1 The normalized absorption spectra of complexes **1**-**4** in different solvents. 6

Fig. S2 HOMO/LUMO orbitals of complexes **1**-**4** based on DFT calculations. 6

Table S1 The photophysical data of complexes **1**-**4** in different solvents. 7

Fig. S3 Photostability of complex **1**-**3** in DCM solution (10 μM) upon irradiation at λ = 400 nm under xenon lamp. 8

Fig. S4 The one-photon and two-photon excited fluorescence spectra of complexes **1**-**4** in THF (20 μM). 9

Fig. S5 The TPEF spectra and the logarithmic plots of the fluorescence integral of **1**-**4** in THF (0.1 mM) at different excitation intensities (mW) at a wavelength of 780 nm. 10

Fig. S6 Plots of one-photon absorption vs. wavelength and two-photon absorption cross-section vs. wavelength for **1**-**4** in DCM. 11

Fig. S7 Plots of one-photon absorption vs. wavelength and two-photon absorption cross-section vs. wavelength for **1**-**4** in THF. 12

Fig. S8 Plots of one-photon absorption vs. wavelength and two-photon absorption cross-section vs. wavelength for **1**-**4** in toluene. 13

Fig. S9 TPA spectra of complexes **1**-**4** in toluene, THF and DCM. 14

Table S2 Single crystal data of complexes **1**-**3**. 15

Fig. S10 The molecular structures of complex **1** viewed along the short and long molecules axis. 16

Fig. S11 The centroid-centroid (Cg-Cg) distances of two adjacent complex **2**. 16

Fig. S12 Molecular stacking of complex **2** along the *c*-axis and the CH⋯F bonding between molecules of adjacent arrays. 17

Fig. S13 Molecular stacking structures of complex **3** along the *a*-axis (top) and *c*-axis (bottom) directions. 17

Fig. S14 The molecular stacking structures of complex **3** and the CH⋯F hydrogen bond between alternative molecules. 18

Table S3 The emission wavelength and the corresponding lifetime at different conditions. 18

Fig. S15 The normalized emission and fluorescence lifetime changes of complexes **1**-**3** upon grinding with different time. 19

Fig. S16 The fluorescence decay profiles of crystal of **1** before and after ground. 20

Fig. S17 The fluorescence decay profiles of crystal of **2** before and after ground. 20

Fig. S18 The fluorescence decay profiles of crystal of **3** before and after ground. 20

Fig. S19 The normalized absorption spectra of complexes **1**-**3** upon grinding of different extent. 21

Fig. S20 (a) The emission spectra of complex **2** in dilute chloroform solution and high concentration chloroform solution (20 mM), λ_{ex} = 405 nm. (b) The fluorescence decay profiles of complex **2** in different conditions. 21

Fig. S21 DSC curves of pristine crystals of **1**-**3**. 21

Fig. S22 Normalized emission spectra of **1**-**3** in pristine crystal and treatment with heating and DCM fuming. 22

Fig. S23 The XRD patterns of complex **1**-**3** in pristine crystal and after grinding-heating process. 22

Fig. S24-S40 The ^{1}H NMR, ^{13}C NMR and HR-MS spectrocospies of chromophores. 23-31

Reference 31

Methods and Materials

Unless otherwise noted, all chemical reagents and solvents were commercially available and were used without further purification. ^{1}H NMR spectra were recorded on a Bruker Avance 400 M spectrometer using tetramethyl silane (TMS) as internal standard at room temperature and referenced to the solvent signal. High resolution mass spectrometry (HR-MS) experiments were performed with Thermo Fisher Q-Exactive or Bruker Apex IV FTMS. UV−visible absorption and emission spectra for the solutions were recorded with Hitachi UV-3900 and F-4600 spectrometer, respectively. Fluorescence quantum yields were determined on Edinburgh instruments FLS-980 with an integrating sphere system. The time-resolved fluorescence spectra were recorded by time-correlated single photon counting (Edinburgh instruments FLS-980), and the values of lifetime were analyzed by exponential function fitting with software F900. Fluorescence microscope images were performed on OLYMPUS IXTI. Powder X-ray diffraction (PXRD) patterns were recorded at room temperature with a Shimadzu XRD-7000. DSC analysis was performed in a Mettler Toledo DSC 1 instrument at heating and cooling rates of 10 °C /min under an N_2 atmosphere.

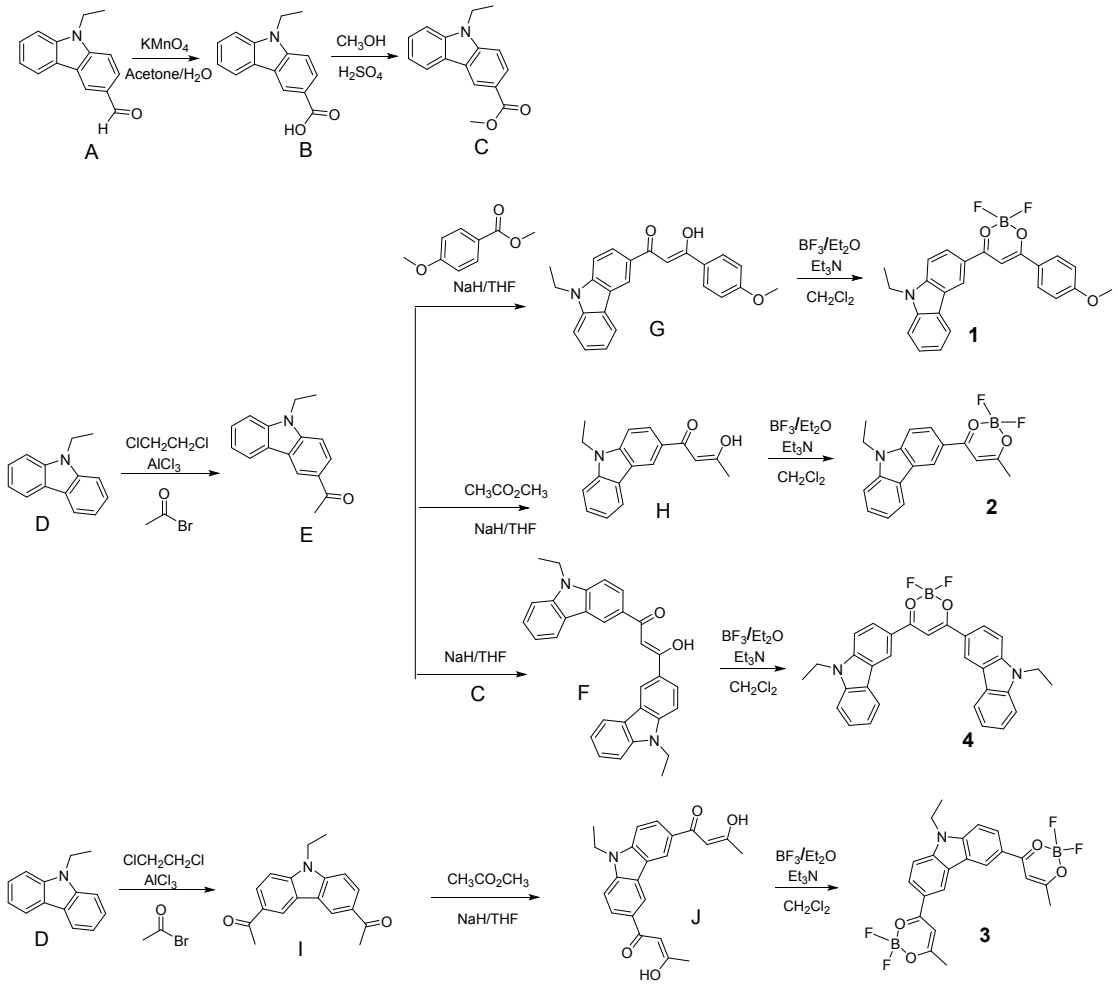

Scheme S1. The synthetic routes of complexes **1**-**4**.

The synthetic routes of complexes **1**-**4** are shown in Scheme 1. The detailed synthetic routes of compounds **B**, **C**, **E**, **F**, and **4** were referred as literature.[S1]

Synthesis of **G**: To a three-necked flask was added compound **E** (475 mg, 2.0 mmol) in 5 mL anhydrous THF. The solution was purged with N_2 for 10 min, and then added NaH (57-63% oil dispersion, 1.0 g, 25 mmol). After stirring for 30 min under N_2 at 65 °C, to the reaction mixture was added methyl 4-methoxybenzoate (332 mg, 2.0 mmol). The reaction mixture was stirred for 24 hours at 65 °C under N_2 protection. After cooling to room temperature, the reaction was quenched by addition of water carefully in an ice bath. The pH was adjusted to 3 with HCl (aq). THF phase was separated, and the aqueous suspension was extracted with dichloromethane. The combined organic phase was dried over anhydrous Na_2SO_4, and concentrated under reduced pressure. The crude product was purified by column chromatography (silica gel, 4:1 v/v, petroleum ether/ethyl acetate) to afford product **G** as orange solid (482 mg, 65%). ^{1}H NMR (400 MHz, $CDCl_3$) δ 17.38 (s, 1H), 8.77 (s, 1H), 8.18 (d, *J* = 8.0 Hz, 1H), 8.12 (d, *J* = 8.0 Hz, 1H), 8.02 (d, *J* = 12.0 Hz, 2H), 7.51 (t, *J* = 8.0 Hz, 1H), 7.46 – 7.41 (d, *J* = 12.0 Hz, 2H), 7.34 – 7.27 (t, *J* = 8.0 Hz, 1H), 7.03 – 6.97 (d, *J* = 12.0 Hz, 2H), 6.92 (s, 1H), 4.39 (q, *J* = 7.2 Hz, 2H), 3.89 (s, 3H), 1.46 (t, *J* = 7.2 Hz, 3H). HR-MS: m/z [M] calculated for $C_{24}H_{21}NO_3$, 371.1521; found, 371.1517.

Synthesis of **1**: To a solution of compound **G** (370 mg, 1.0 mmol) in 5 mL CH_2Cl_2 was added Et_3N (500 µL, 3.6 mmol). After stirring for 10 min at room temperature, BF_3/Et_2O (400 µL, 3.0 mmol) was added. The solution was stirred for another 2 hours in the dark. Water was added to the solution, and the organic layers was collected, washed with saturated $NaHCO_3$ solution and brine, dried over anhydrous Na_2SO_4, and concentrated under reduced pressure. The crude product was purified by column chromatography (silica gel, 1:1 v/v, petroleum ether/dichloromethane) to afford product **1** as yellow solid (350 mg, 83%). ^{1}H NMR (600 MHz, DMSO-d_6) δ 9.25 (s, 1H), 8.42 (d, *J* = 8.9 Hz, 1H), 8.36 – 8.34 (m, 3H), 7.86 (s, 1H), 7.81 (d, *J* = 8.8 Hz, 1H), 7.71 (d, *J* = 8.2 Hz, 1H), 7.54 (t, *J* = 7.5 Hz, 1H), 7.33 (t, *J* = 7.4 Hz, 1H), 7.18 (d, *J* = 8.9 Hz, 2H), 4.52 (q, *J* = 7.1 Hz, 2H), 3.90 (s, 3H), 1.34 (t, *J* = 7.1 Hz, 3H). ^{13}C NMR (101 MHz, DMSO-d_6) δ 181.7, 179.3, 165.5, 144.4, 141.0, 132.0, 127.7, 127.6, 124.5, 123.9, 123.4, 122.9, 122.2, 121.6, 121.2, 115.3, 110.7, 110.50, 92.9, 56.4, 38.1, 14.3. HR-MS: m/z [M + H] calculated for $C_{24}H_{21}BF_2NO_3$, 420.1583; found, 420.1585.

Synthesis of **H**: To a three-necked flask was added compound **E** (500 mg, 2.1 mmol) in 5 mL anhydrous THF. The solution was purged with N_2 for 10 min, and then added NaH (57-63% oil dispersion, 0.5 g, 12 mmol). After stirring for 30 min under N_2 at 65 °C, to the reaction mixture was added methyl acetate (0.5 mL, 6.2 mmol). The reaction mixture was stirred for 24 hours at 65 °C under N_2 protection. After cooling to room temperature, the reaction was quenched by addition of water carefully in an ice bath. The pH was adjusted to 3 with HCl (aq). THF phase was separated, and the aqueous suspension was extracted with dichloromethane. The combined organic phase was dried over anhydrous Na_2SO_4, and concentrated under reduced pressure. The crude product was purified by column chromatography (silica gel, 10:1 v/v, petroleum ether/ethyl acetate) to afford product **H** as yellow oil (310 mg, 54%). ^{1}H NMR (400 MHz, $CDCl_3$) δ 16.57 (s, 1H), 8.70 (d, *J* = 1.5 Hz, 1H), 8.16 (d, *J* = 7.7 Hz, 1H), 8.04 (dd, *J* = 8.7, 1.8 Hz, 1H), 7.52 (t, *J* = 8.0 Hz, 1H), 7.43 (t, *J* = 8.0 Hz, 2H), 7.34 – 7.27 (t, *J* = 8.0 Hz, 1H), 6.33 (s, 1H), 4.39 (q, *J* = 7.2 Hz, 2H), 2.23 (s, 3H), 1.46 (t, *J* = 7.2 Hz, 4H). HR-MS: m/z [M + H] calculated for $C_{18}H_{18}NO_2$, 280.1338; found, 280.1329.

Synthesis of **2**: To a solution of compound **H** (300 mg, 1.1 mmol) in 5 mL CH_2Cl_2 was added Et_3N (500 µL, 3.6 mmol). After stirring for 10 min at room temperature, BF_3/Et_2O (400 µL, 3.0 mmol) was added. The solution was stirred for another 2 hours in the dark. Water was added to the solution, and the organic layers was collected, washed with saturated $NaHCO_3$ solution and brine, dried over anhydrous Na_2SO_4, and concentrated under reduced pressure. The crude product was purified by column chromatography (silica gel, 1:1 v/v, petroleum ether/dichloromethane) to afford product **2** as yellow solid (40 mg, 80%). ^{1}H NMR (400 MHz, $CDCl_3$) δ 8.87 (d, *J* = 1.7 Hz, 1H), 8.17 – 8.14 (d, *J* = 8.0 Hz, 2H), 7.59 – 7.53 (d, *J* = 8.0 Hz, 1H), 7.45 (dd, *J* = 11.6, 8.0 Hz, 2H), 7.36 (t, *J* = 8.0 Hz, 1H), 6.64 (s, 1H), 4.40 (q, *J* = 7.3 Hz, 2H), 2.40 (s, 3H), 1.48 (t, *J* = 7.3 Hz, 3H). ^{13}C NMR (101 MHz, $CDCl_3$) δ 188.6, 182.7, 144.4, 140.8, 127.2, 127.1, 123.6, 123.2, 122.9, 121.2, 121.0, 121.0, 109.4, 108.9, 96.5, 38.1, 24.4, 13.9.HR-MS: m/z [M + NH_4] calculated for $C_{18}H_{20}BF_2N_2O_2$, 345.1586; found, 345.1581.

Synthesis of **I**: To a solution of **D** (400 mg, 2.1 mmol) in 6 mL 1,2-dichloroethane was added $AlCl_3$ (2.0 g, 15 mmol) and acetyl bromide (500 µL, 6.0 mmol). The reaction mixture was stirred at room temperature for 5 hours, and then poured into 20 mL diluted HCl ice water. The organic phase was collected, dried over anhydrous Na_2SO_4 and concentrated in vacuum. The crude product was purified by column chromatography (silica gel, 1:1 v/v, petroleum ether/dichloromethane) to afford **D** as grey

solid (510 mg, 89%).^{1}H NMR (400 MHz, $CDCl_3$) δ 8.70 (s, 2H), 8.11 (d, *J* = 8.0 Hz, 2H), 7.41 (d, *J* = 8.0 Hz, 1H), 4.39 (q, *J* = 7.2 Hz, 2H), 2.70 (s, 6H), 1.46 (t, *J* = 7.2 Hz, 3H). HR-MS: m/z [M] calculated for $C_{18}H_{17}NO_2$, 279.1259; found, 279.1260.

Synthesis of **J**: To a three-necked flask was added compound **I** (560 mg, 2.0 mmol) in 5 mL anhydrous THF. The solution was purged with N_2 for 10 min, and then added NaH (57-63% oil dispersion, 1.0 g, 25 mmol). After stirring for 30 min under N_2 at 65 °C, to the reaction mixture was added methyl acetate (1.0 mL, 12 mmol). The reaction mixture was stirred for 24 hours at 65 °C under N_2 protection. After cooling to room temperature, the reaction was quenched by addition of water carefully in an ice bath. The pH was adjusted to 3 with HCl (aq). THF phase was separated, and the aqueous suspension was extracted with dichloromethane. The combined organic phase was dried over anhydrous Na_2SO_4, and concentrated under reduced pressure. The crude product was purified by column chromatography (silica gel, 10:1 v/v, petroleum ether/ethyl acetate) to afford product **J** as green-yellow solid (250 mg, 34%). ^{1}H NMR (400 MHz, $CDCl_3$) δ 16.49 (s, 2H), 8.73 (s, 1H), 8.09 (d, *J* = 8.5 Hz, 2H), 7.46 (d, *J* = 8.5 Hz, 2H),6.34 (s, 2H), 4.43 (q, *J* = 7.2 Hz, 4H), 2.24 (s, 6H), 1.48 (t, *J* = 7.2 Hz, 6H). HR-MS: m/z [M + Na] calculated for $C_{22}H_{21}NaNO_4$, 386.1368; found, 386.1361.

Synthesis of **3**: To a solution of compound **J** (360 mg, 1.0 mmol) in 5 mL CH_2Cl_2 was added Et_3N (1.0 mL, 7.2 mmol). After stirring for 10 min at room temperature, BF_3/Et_2O (800 µL, 6.0 mmol) was added. The solution was stirred for another 2 hours in the dark. Water was added to the solution, and the organic layers was collected, washed with saturated $NaHCO_3$ solution and brine, dried over anhydrous Na_2SO_4, and concentrated under reduced pressure. The crude product was purified by column chromatography (silica gel, 1:1 v/v, petroleum ether/dichloromethane) to afford product **3** as yellow solid (373 mg, 81%). ^{1}H NMR (600 MHz, DMSO-d_6) δ 9.24 (s, 2H), 8.29 (d, *J* = 8.8 Hz, 2H), 7.87 (d, *J* = 8.8 Hz, 2H), 7.30 (s, 2H), 4.54 (q, *J* = 7.1 Hz, 2H), 2.43 (s, 3H), 1.34 (t, *J* = 7.2 Hz, 3H). ^{13}C NMR (101 MHz, DMSO-d_6) δ 191.6, 181.9, 145.4, 128.5, 124.5, 123.4, 123.0, 111.6, 97.9, 38.6, 24.7, 14.3. HR-MS: m/z [M + NH_4] calculated for $C_{22}H_{23}B_2F_4N_2O_4$, 477.1780; found, 477.1774.

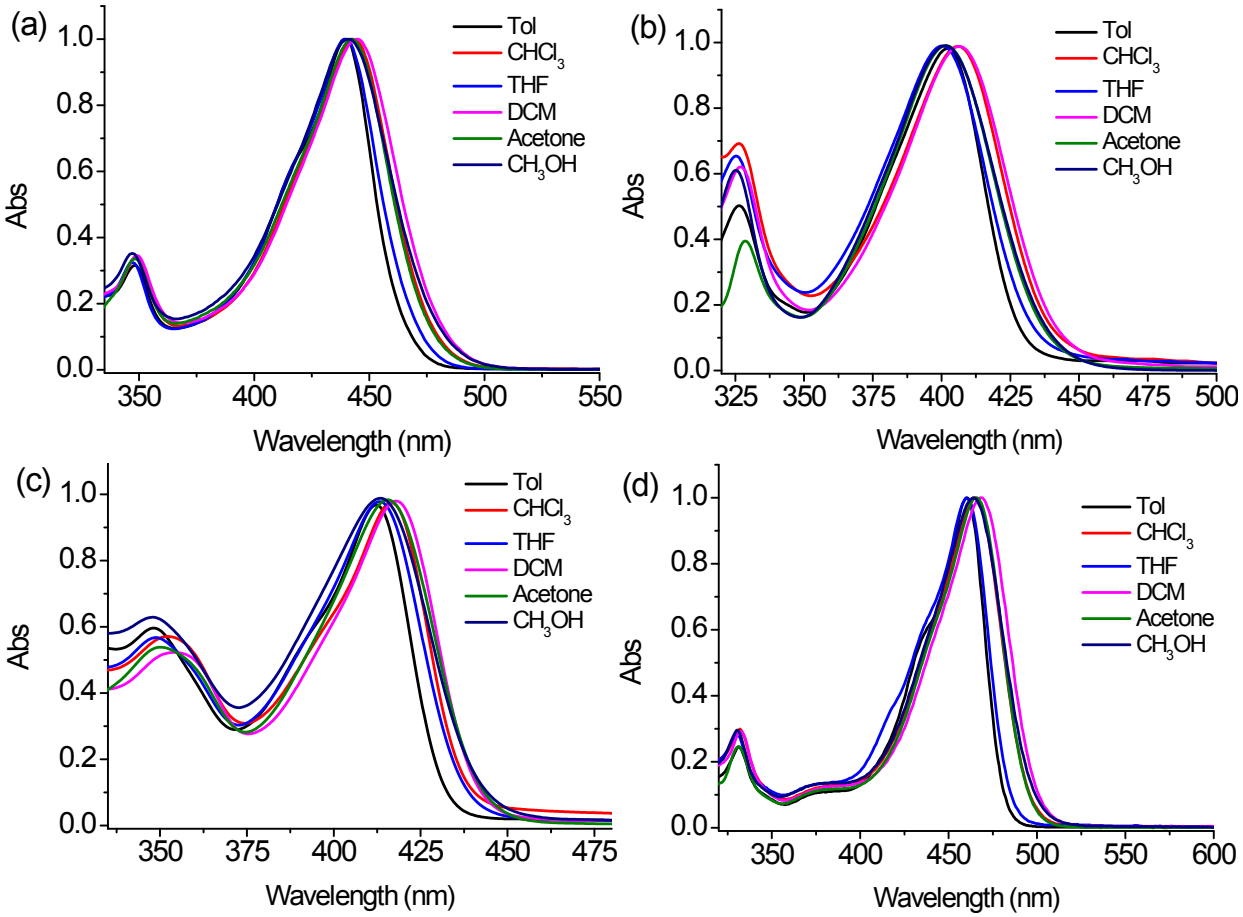

Fig. S1 The normalized absorption spectra of complexes **1** (a), **2** (b), **3** (c) and **4** (d) in different solvents.

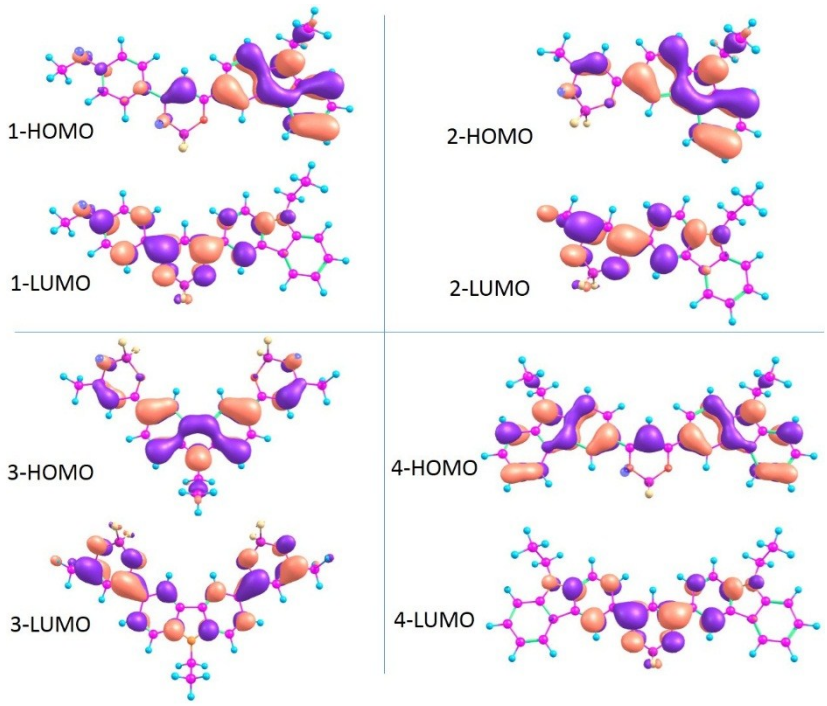

Fig. S2 HOMO/LUMO orbitals of complexes **1**-**4** based on DFT calculations.

Table S1 The photophysical data of complexes **1**-**4** in different solvents.

	Solvents	[a] λ_{abs}/nm	[b] ε/ $cm^{-1}M^{-1}$	[c] λ_{em}/nm	[d] Φ_f	[e] τ_f/ns	[f] k_f/ 10^9 S^{-1}	[g] k_{nr}/ 10^9 S^{-1}
	Toluene	440	72000	474	0.93	2.26	0.41	0.03
1	**$CHCl_3$**	443	75300	495	0.89	3.00	0.30	0.04
	THF	440	82670	498	0.91	3.48	0.26	0.03
	DCM	445	69300	514	0.84	3.92	0.21	0.04
	Acetone	442	69000	521	0.48	3.07	0.16	0.17
	CH_3OH	441	53000	530	0.07	0.94	0.07	0.99
	Toluene	402	44000	444	0.87	3.43	0.25	0.04
2	**$CHCl_3$**	406	51950	475	0.75	4.83	0.15	0.05
	THF	400	47800	475	0.79	5.36	0.15	0.04
	DCM	406	46000	495	0.70	6.00	0.12	0.05
	Acetone	402	46200	506	0.57	5.80	0.10	0.07
	CH_3OH	401	40400	534	0.05	0.64	0.08	1.48
	Toluene	412	60800	436	0.88	2.00	0.44	0.06
3	**$CHCl_3$**	417	67400	443	0.92	2.11	0.44	0.04
	THF	414	61800	450	0.95	2.52	0.38	0.02
	DCM	418	54400	451	0.93	2.50	0.37	0.03
	Acetone	417	59000	460	0.81	3.30	0.25	0.06
	CH_3OH	414	52800	476	0.39	3.48	0.11	0.18
	Toluene	460	75600	481	0.93	1.87	0.50	0.04
4	**$CHCl_3$**	466	93600	504	0.89	1.95	0.46	0.06
	THF	460	108200	489	0.93	2.14	0.43	0.03
	DCM	467	101300	513	0.80	2.12	0.38	0.09
	Acetone	464	105600	506	0.81	2.45	0.33	0.08
	CH_3OH	463	39100	525	0.40	1.98	0.20	0.30

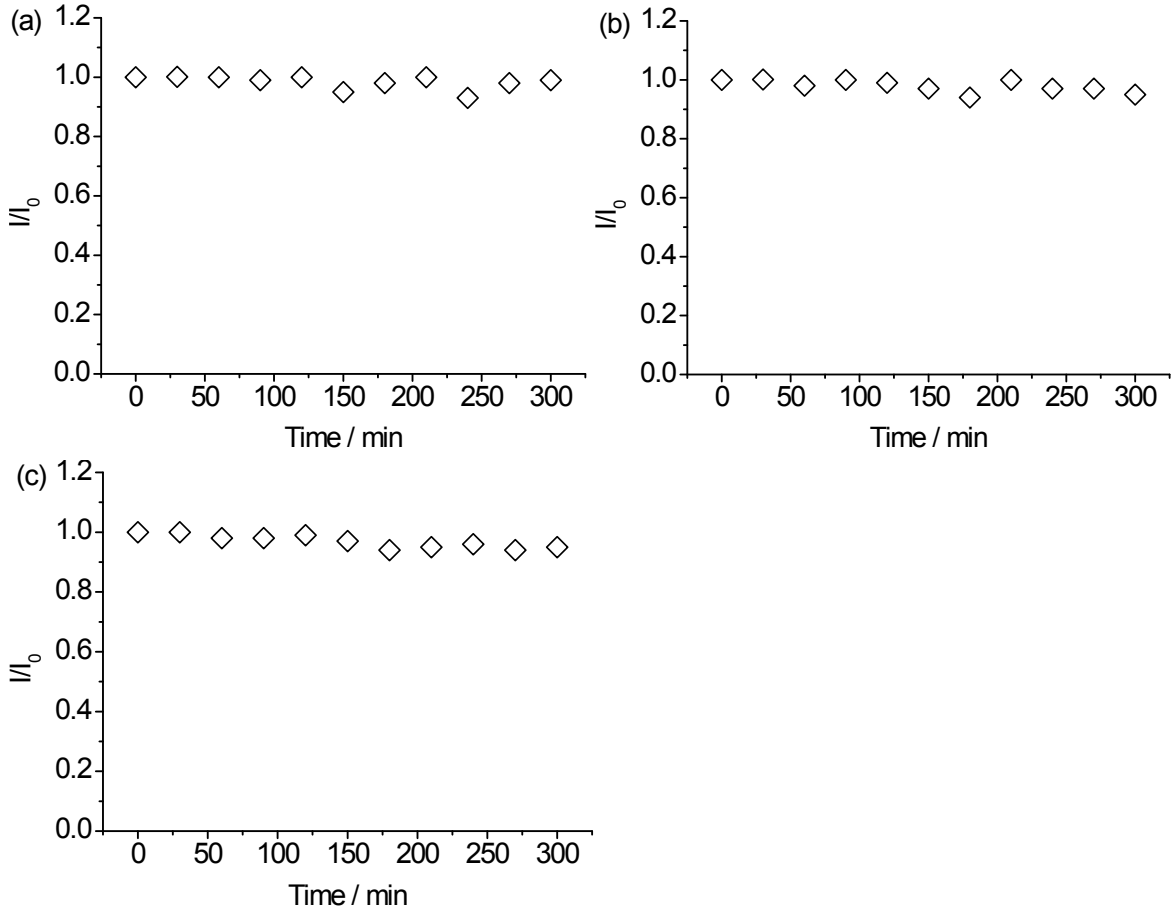

Fig. S3 Photostability of complex **1** (a), **2** (b) and **3** (c) in DCM solution (10 μM) upon irradiation at λ = 400 nm under xenon lamp.

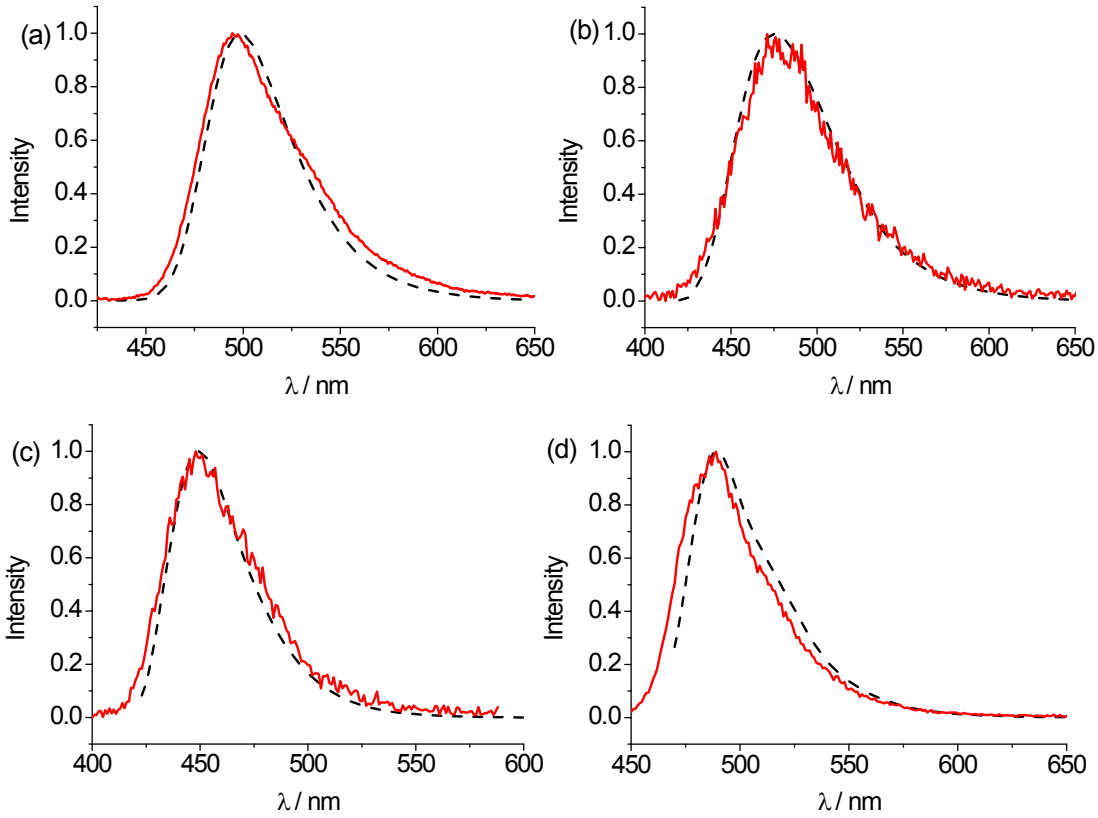

Fig. S4 The one-photon (black dashed line) and two-photon (red solid line) excited fluorescence spectra of complexes **1**(a), **2**(b), **3**(c) and **4**(d) in THF (20 μM).

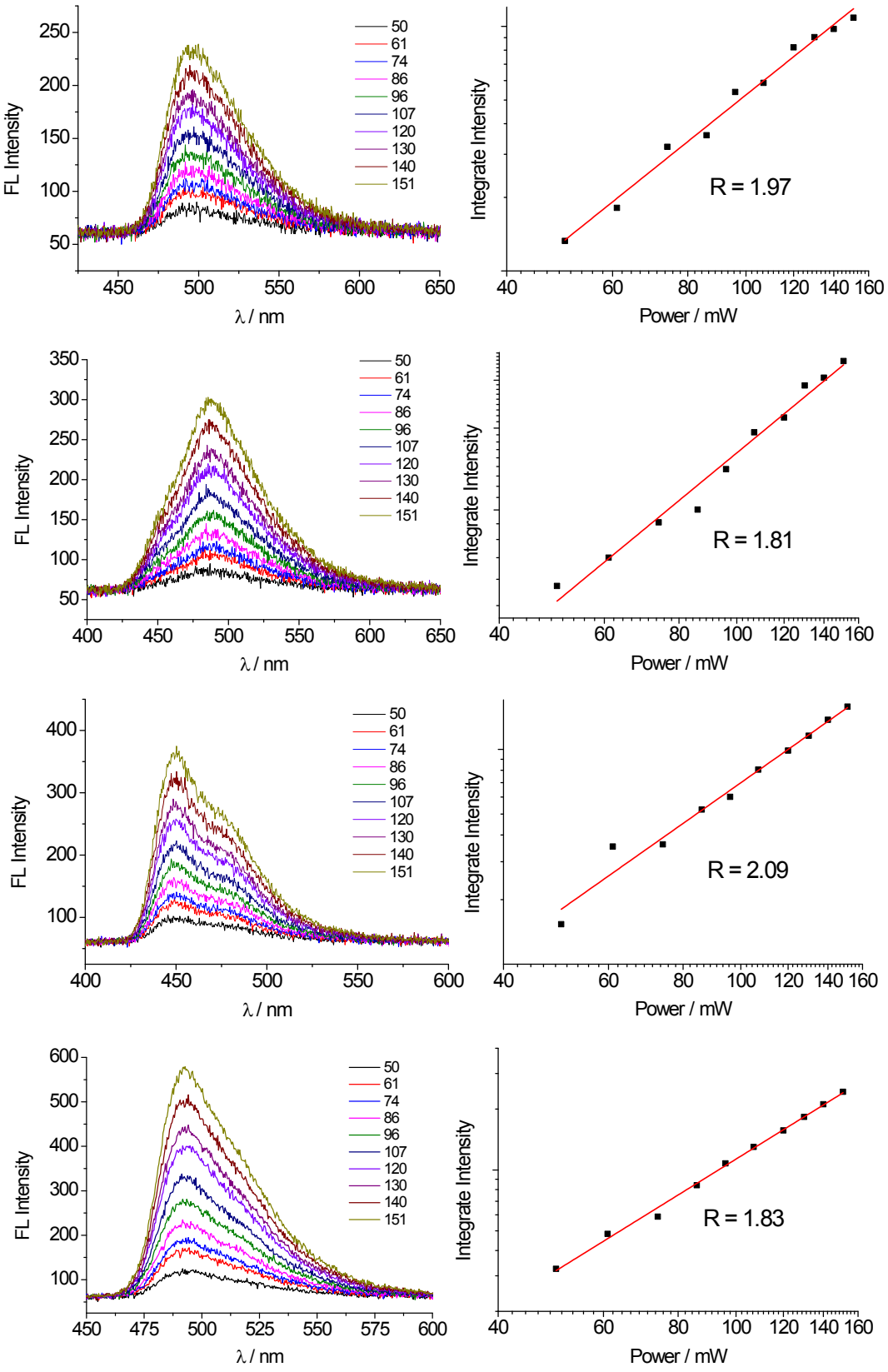

Fig. S5 The TPEF spectra and the logarithmic plots of the fluorescence integral of **1**-**4** in THF (0.1 mM) at different excitation intensities (mW) at a wavelength of 780 nm.

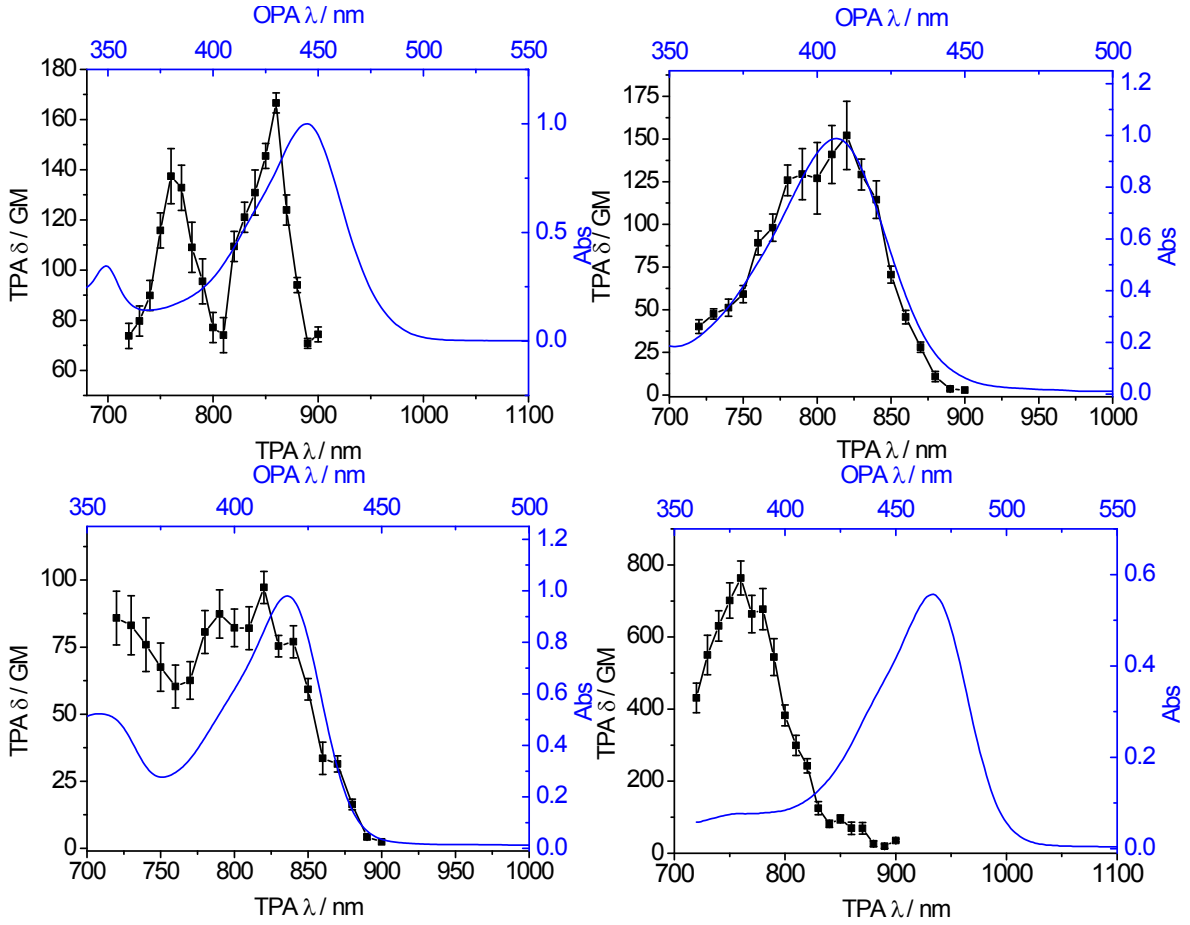

Fig. S6 Plots of one-photon absorption vs. wavelength (blue lines, right-hand side and top axes) and two-photon absorption cross-section vs. wavelength (filled squares, left-hand side and bottom axes) for **1**-**4** in DCM.

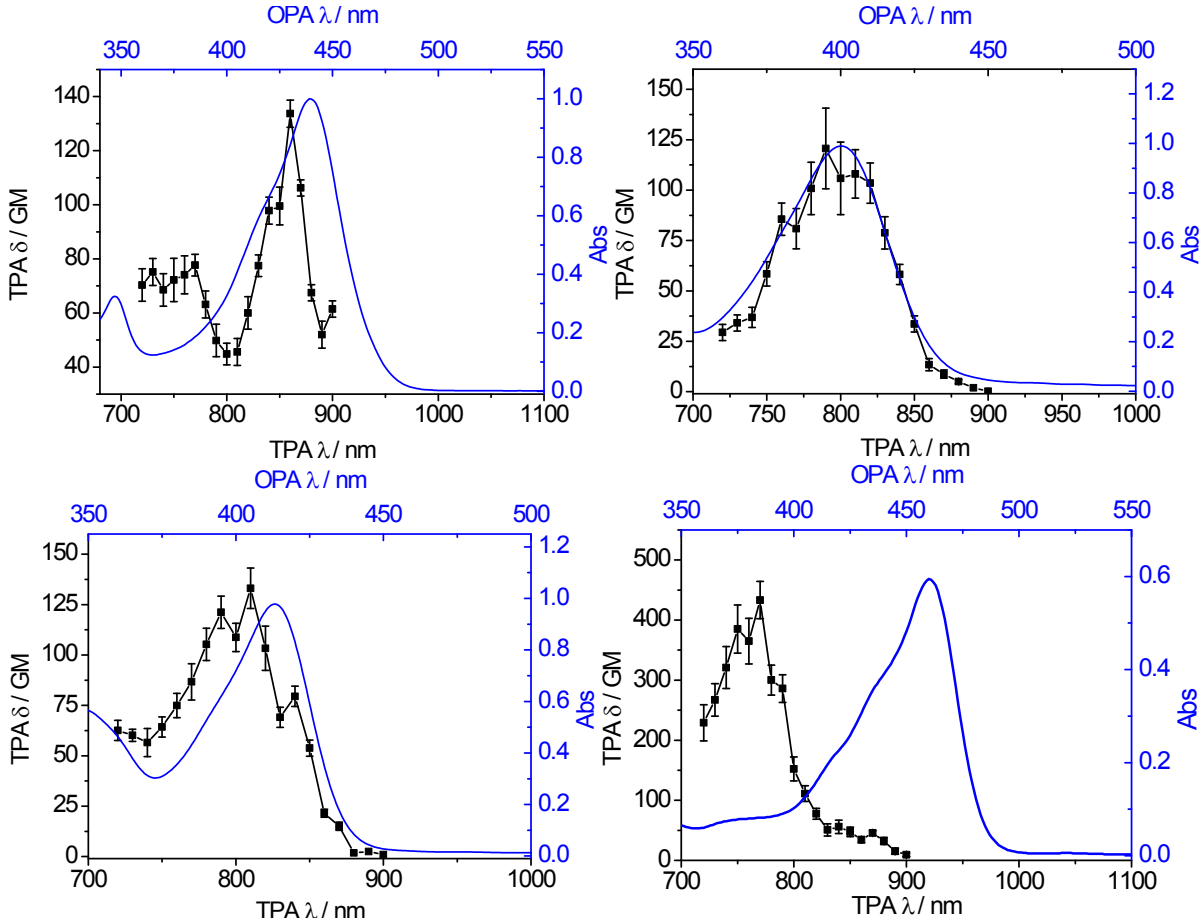

Fig. S7 Plots of one-photon absorption vs. wavelength (blue lines, right-hand side and top axes) and two-photon absorption cross-section vs. wavelength (filled squares, left-hand side and bottom axes) for **1**-**4** in THF.

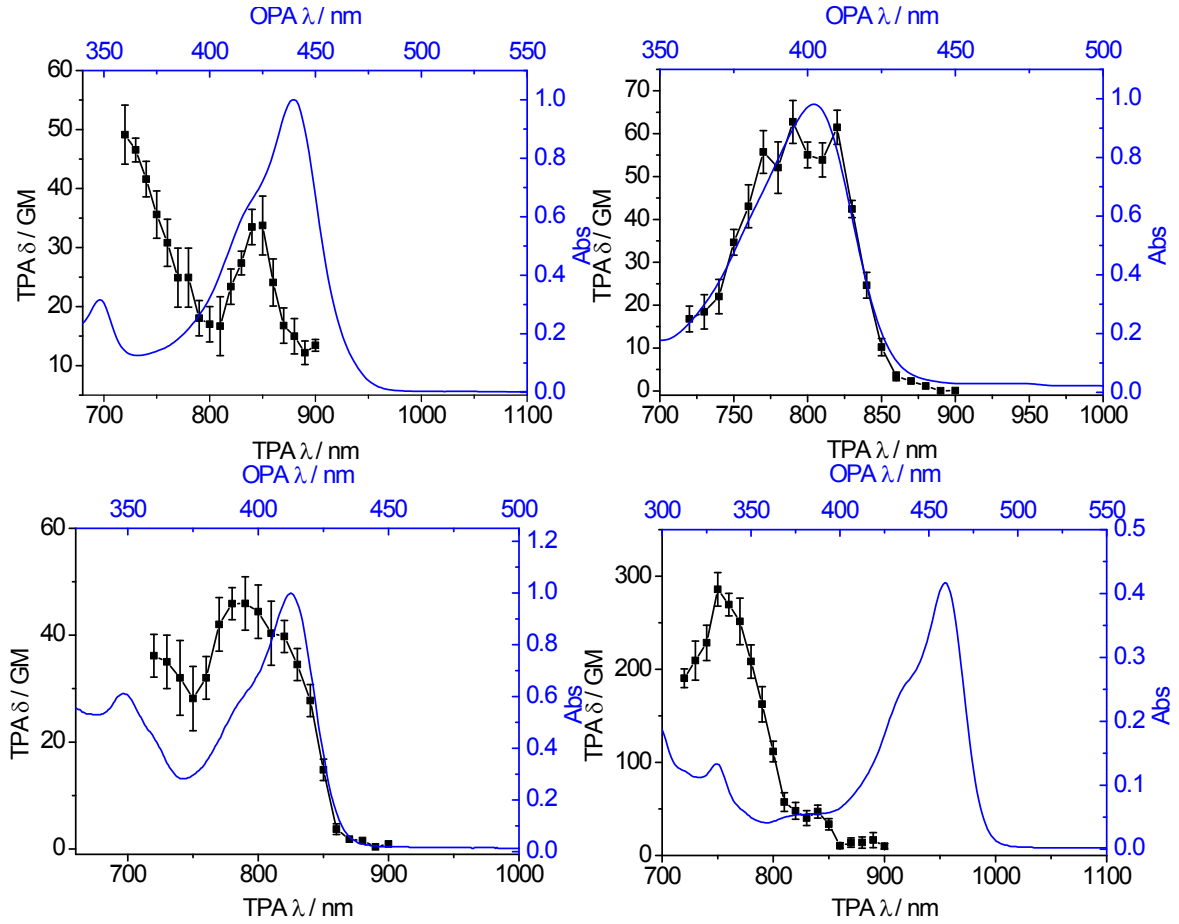

Fig. S8 Plots of one-photon absorption vs. wavelength (blue lines, right-hand side and top axes) and two-photon absorption cross-section vs. wavelength (filled squares, left-hand side and bottom axes) for **1**-**4** in toluene.

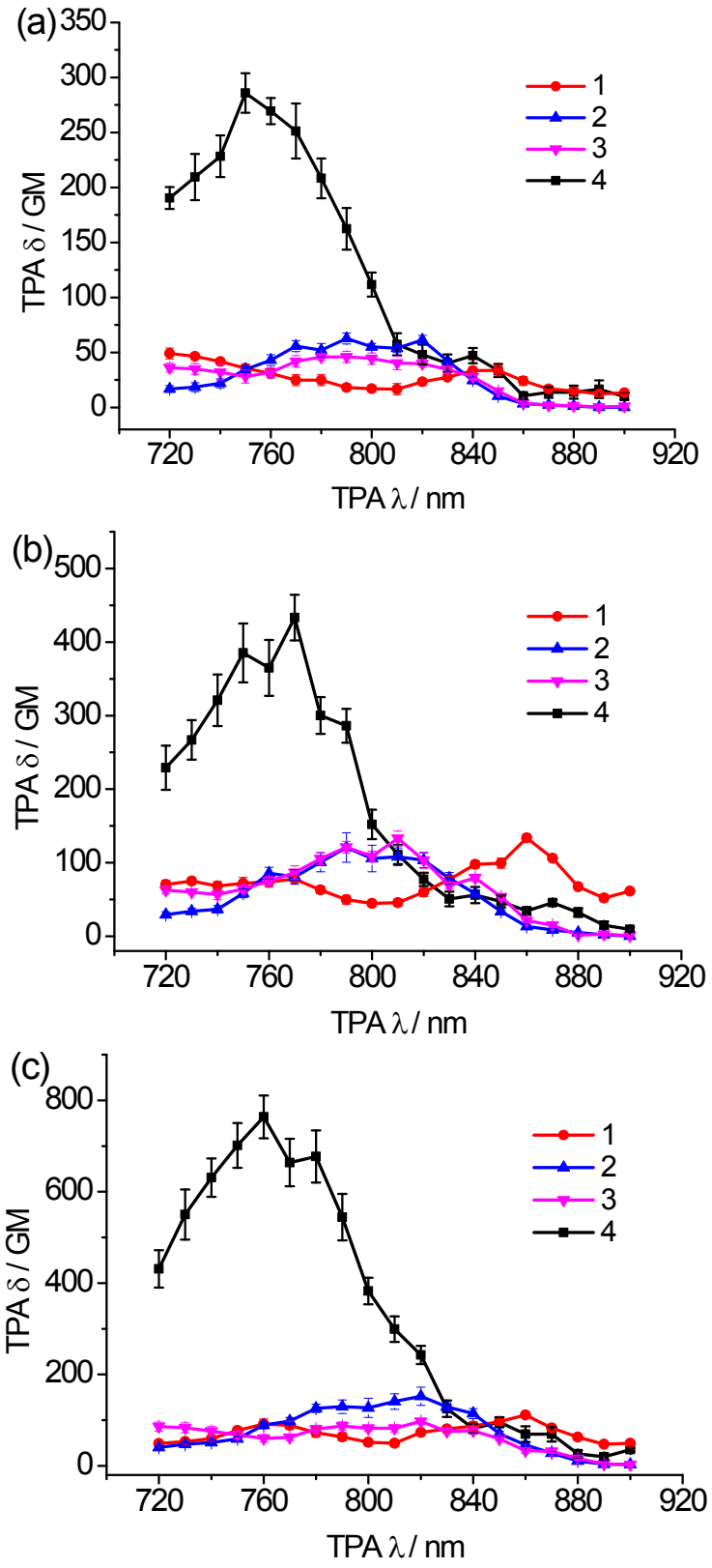

Fig. S9 TPA spectra of complexes **1**-**4** in toluene (a), THF (b) and DCM (c).

Table S2 Single crystal data of complexes **1**-**3**.

	1	**2**	**3**
CCDC number	1574740	1574741	1574742
Empirical formula	$C_{24}H_{20}BNO_3F_2$	$C_{18}H_{16}BNO_2F_2$	$C_{22}H_{19}B_2F_4NO_4$
Formula weight	419.22	327.13	459.00
Temperature/K	153.15	153.15	100.01
Crystal system	Monoclinic	Monoclinic	tetragonal
Space group	$P2_1/n$	C2/c	$P4_2/n$
Unit cell dimensions	a = 11.151 (2) Å b = 13.828 (3) Å c = 13.934 (3) Å α= 90° β = 112.20(3) ° γ = 90°	a = 21.231(4) Å b = 9.2009(18) Å c = 16.416(3) Å α = 90° β = 105.76(3)° γ = 90°	a = 23.179(3) Å b = 23.179(3) Å c = 7.6814(15) Å α = 90° β = 90 ° γ = 90°
Volume ($Å^3$)	1989.2(8)	3086.2(11)	4127.0(11)
Z	4	8	8
ρ_{calc} g/cm^3	1.400	1.408	1.477
μ/mm^{-1}	0.104	0.107	0.123
F(000)	872.0	1360.0	1888.0
Radiation	MoKα (λ = 0.71073)	MoKα (λ = 0.71073)	MoKα (λ = 0.71073)
2Θ range for data collection/°	4.318 to 54.972	5.156 to 54.916	5.86 to 49.98
Index ranges	-14 ≤ h ≤ 14, -17 ≤ k ≤ 17, -18 ≤ l ≤ 18	-20 ≤ h ≤ 27, -11 ≤ k ≤ 11, -21 ≤ l ≤ 21	-27 ≤ h ≤ 27, -27 ≤ k ≤ 27, -9 ≤ l ≤ 9
Reflections collected	13400	12172	26668
Independent reflections	4488 [R_{int} = 0.0471, R_{sigma} = 0.0499]	3513 [R_{int} = 0.0545, R_{sigma} = 0.0487]	3596 [R_{int} = 0.0748, R_{sigma} = 0.0408]
Goodness-of-fit on F^2	1.238	1.261	1.392
Final R indices [I>2sigma(I)]	R_1 = 0.0962, wR2 = 0.1763	R_1 = 0.0839, wR_2 = 0.1489	R_1 = 0.0910, wR_2 = 0.1412
R indices (all data)	R_1 = 0.1116, wR2 = 0.1853	R_1 = 0.1001, wR_2 = 0.1722	R_1 = 0.0955, wR_2 = 0.1425

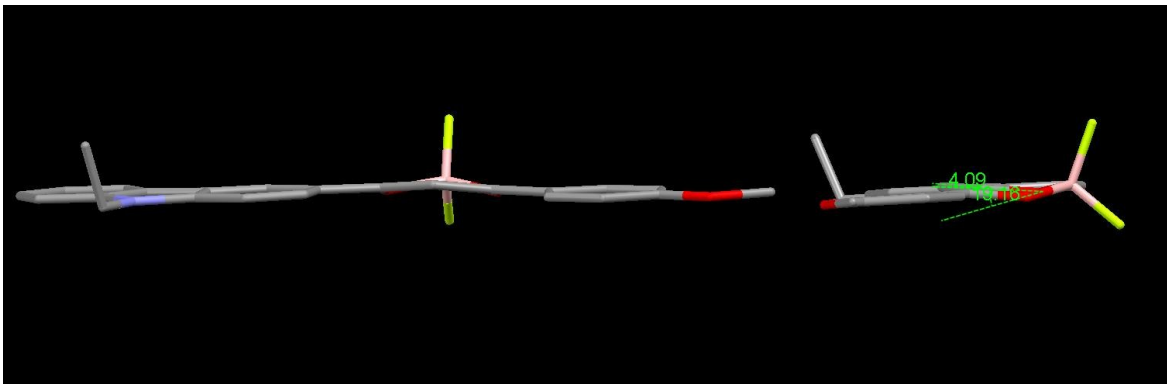

Fig. S10 The molecular structures of complex **1** viewed along the short and long molecules axis.

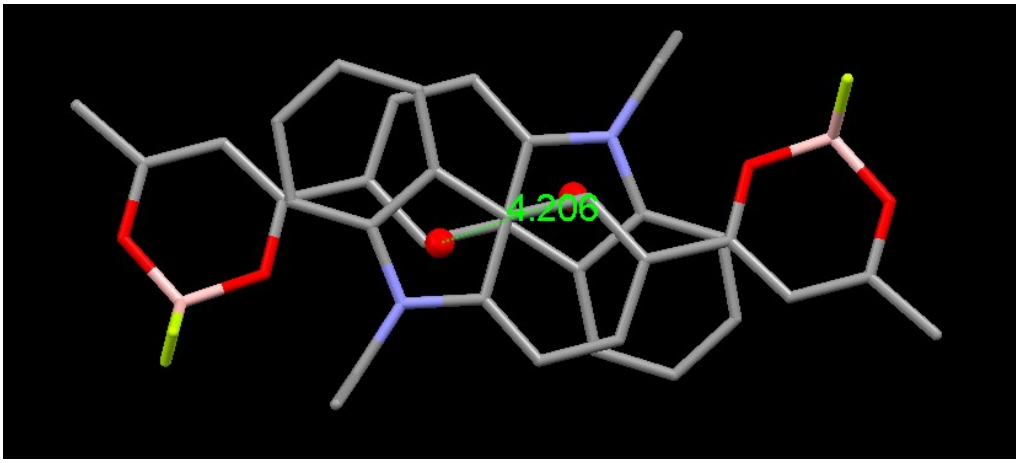

Fig. S11 The centroid-centroid (Cg-Cg) distances of two adjacent complex **2**.

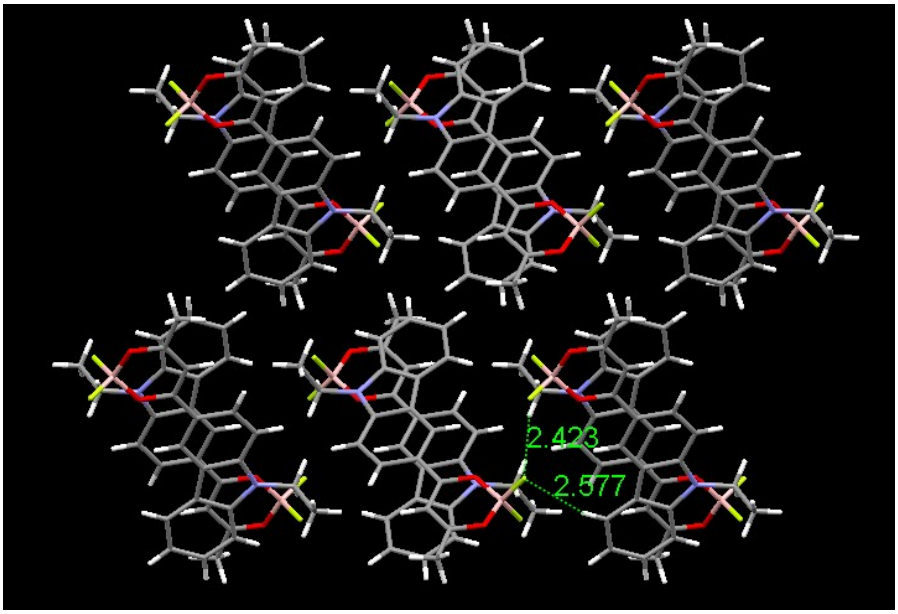

Fig. S12 Molecular stacking of complex **2** along the *c*-axis direction and the CH⋯⋯F hydrogen bonding between molecules of adjacent arrays.

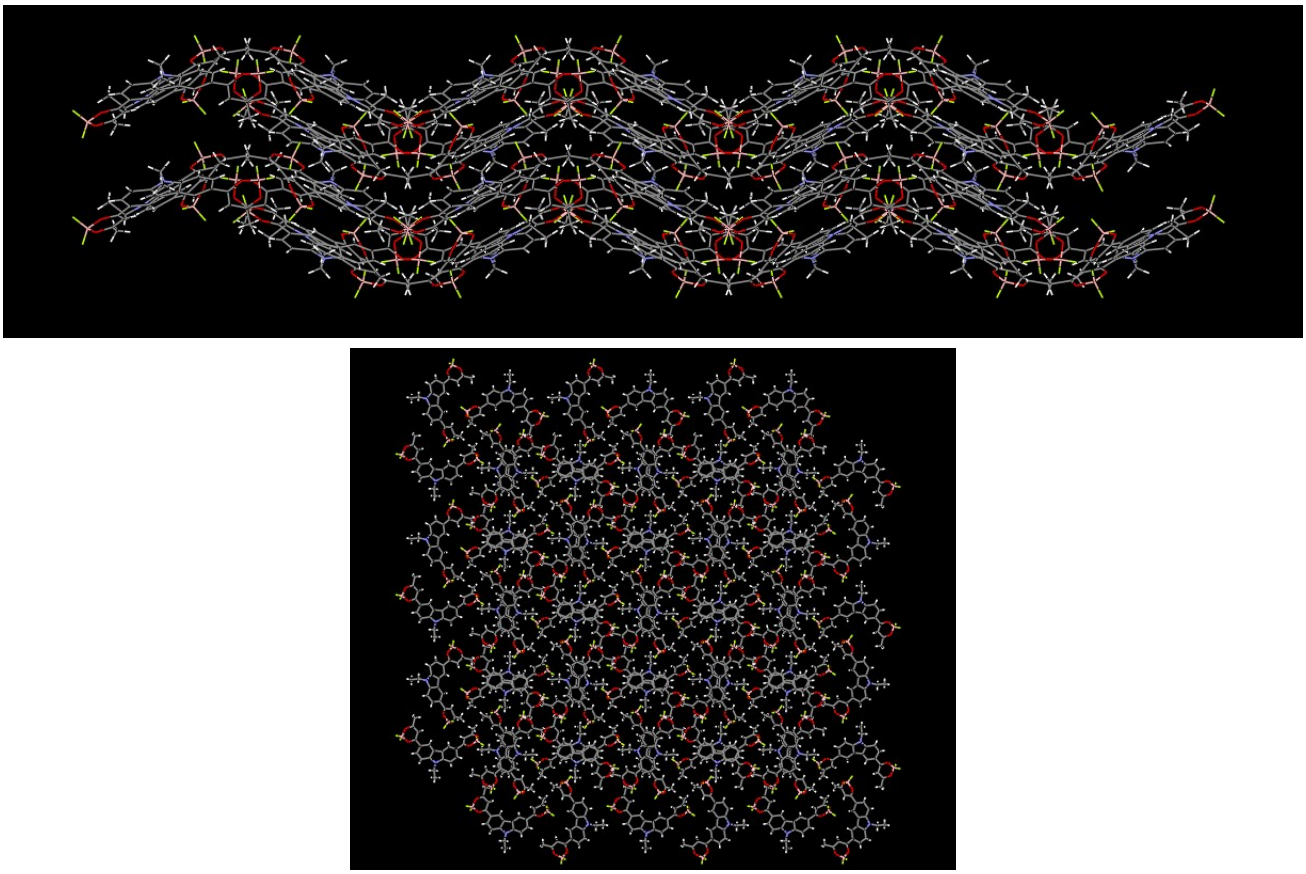

Fig. S13 Molecular stacking structures of complex **3** along the *a*-axis (top) and *c*-axis (bottom) directions.

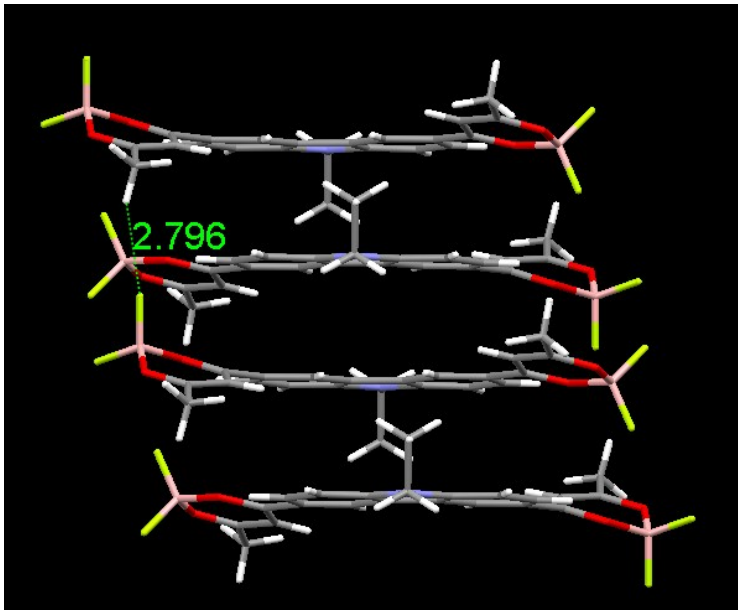

Fig. S14 The molecular stacking structures of complex **3** and the CH···F hydrogen bonding between alternative molecules.

Table S3 The emission wavelength and the corresponding lifetime at different conditions.

	1	**2**	**3**
pristine	**λ_{em} = 627 nm** 2.1 ns, 21.0%; 5.3 ns, 71.0%; 19.9 ns, 8.0%	**λ_{em} = 566 nm** 3.1 ns, 96.7%; 9.0 ns, 3.3%	**λ_{em} = 542 nm** 1.4 ns, 40.34%; 3.8 ns, 37.5%; 16.7 ns, 22.1%
Partly ground	**λ_{em} = 612 nm** 2.6 ns, 35.0%; 5.7 ns, 54.0%; 17.7 ns, 11.0% **λ_{em} = 557 nm** (shoulder peak) 0.6 ns, 44.0%; 1.4 ns, 41.0%; 6.4 ns, 15.0%	**λ_{em} = 553 nm** 3.0 ns, 96.0%; 8.7 ns, 4.0% **λ_{em} = 535 nm** (shoulder peak) 1.62ns, 62.2%; 4.72 ns, 37.8%	**λ_{em} = 499 nm** 0.5 ns, 40.2%; 1.4 ns, 41.0%; 8.5 ns, 18.8 % **λ_{em} = 528 nm** (shoulder peak) 1.0 ns, 26.5%; 2.8 ns, 54.0%; 13.1 ns, 19.5%
Fully ground	**λ_{em} = 597 nm** 2.9 ns, 15.0%; 10.1 ns, 49.0%; 24.3 ns, 36.0%	**λ_{em} = 535 nm** 1.45 ns, 63.1% 5.60 ns, 36.9%	**λ_{em} = 556 nm** 0.7 ns, 19.6%; 1.7 ns, 53.9%; 5.0 ns, 26.5%
ground-heating	**λ_{em} = 535 nm** 0.6 ns, 70.3%; 4.2 ns, 29.7%	**λ_{em} = 518 nm** 1.9 ns, 63.0%; 3.8 ns, 37.0%	**λ_{em} = 526 nm** 1.5 ns, 50.9%; 4.4 ns, 49.1%

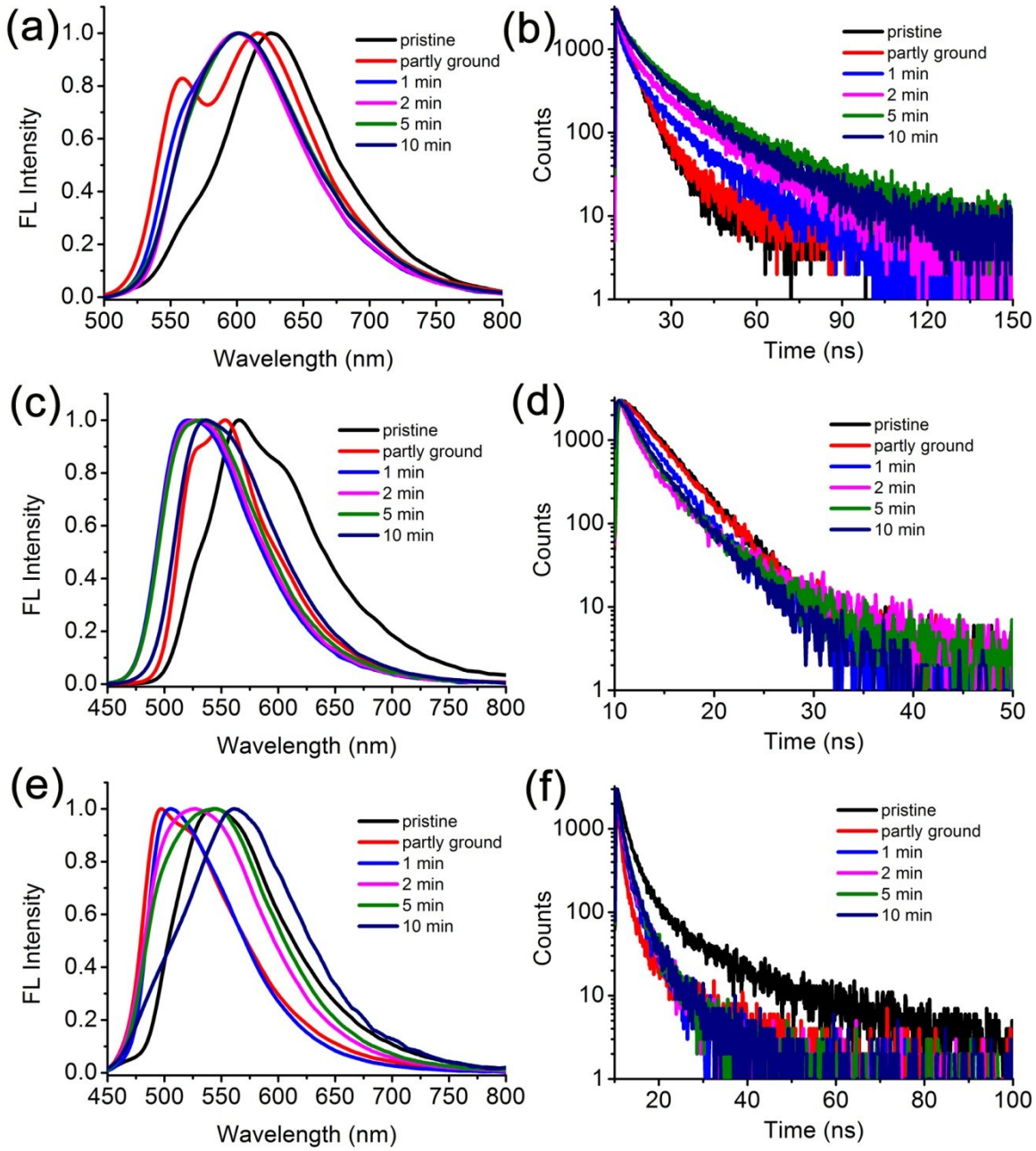

Fig. S15 The normalized emission and fluorescence lifetime (monitored at emission maximum) changes of complexes **1**(a, b), **2**(c, d) and **3**(e, f) upon grinding with different time.

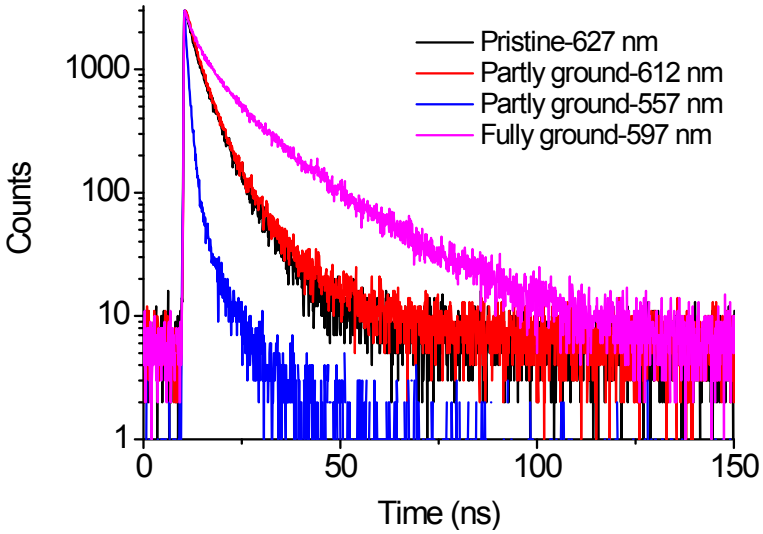

Fig. S16 The fluorescence decay profiles of crystal of **1** before and after ground.

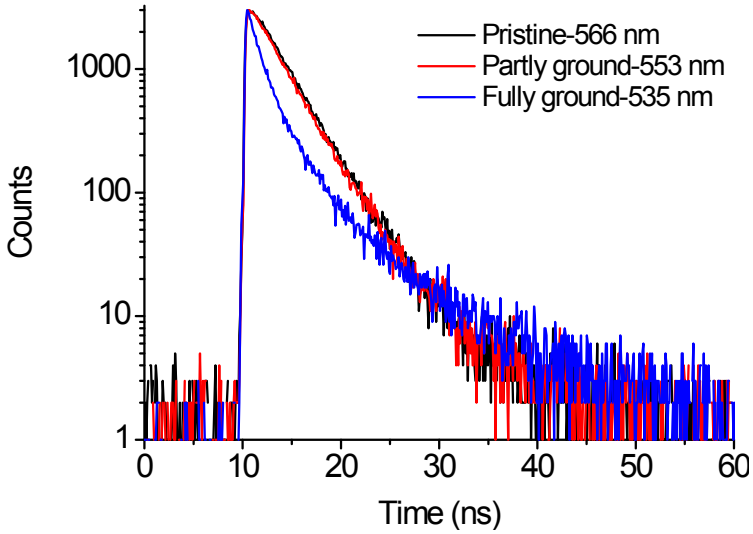

Fig. S17 The fluorescence decay profiles of crystal of **2** before and after ground.

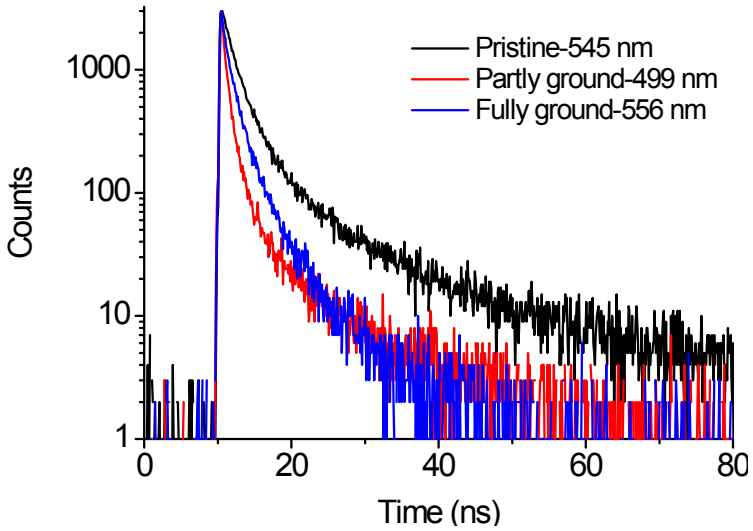

Fig. S18 The fluorescence decay profiles of crystal of **3** before and after ground.

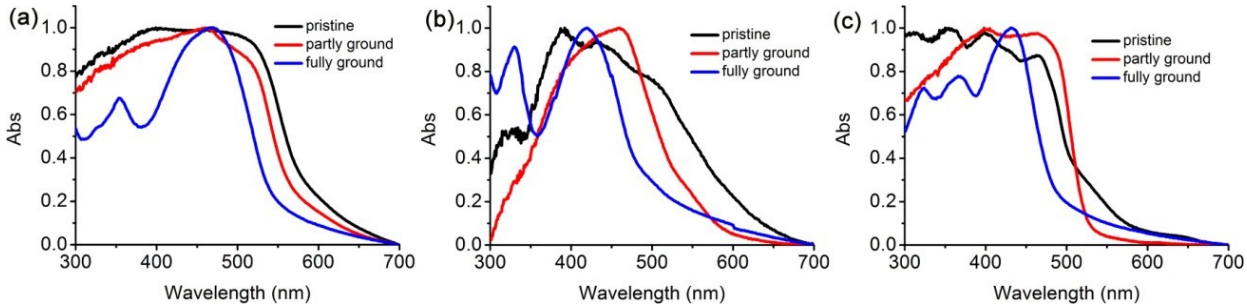

Fig. S19 The normalized absorption spectra of complexes 1(a), 2(b) and 3(c) upon grinding of different extent.

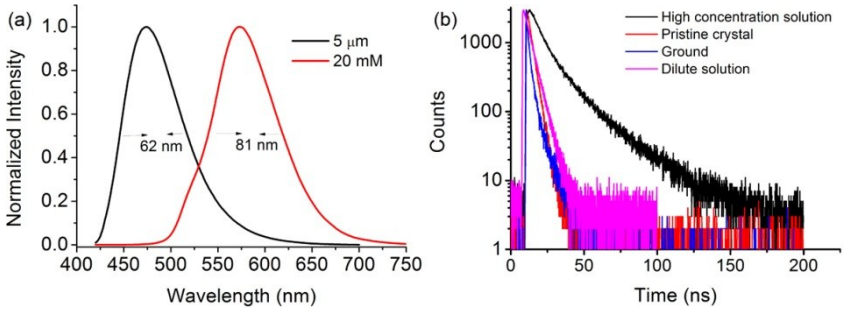

Fig. S20 (a) The emission spectra of complex **2** in dilute chloroform solution (5 μM) and high concentration chloroform solution (20 mM), λ_{ex} = 405 nm. (b) The fluorescence decay profiles of complex **2** in different conditions.

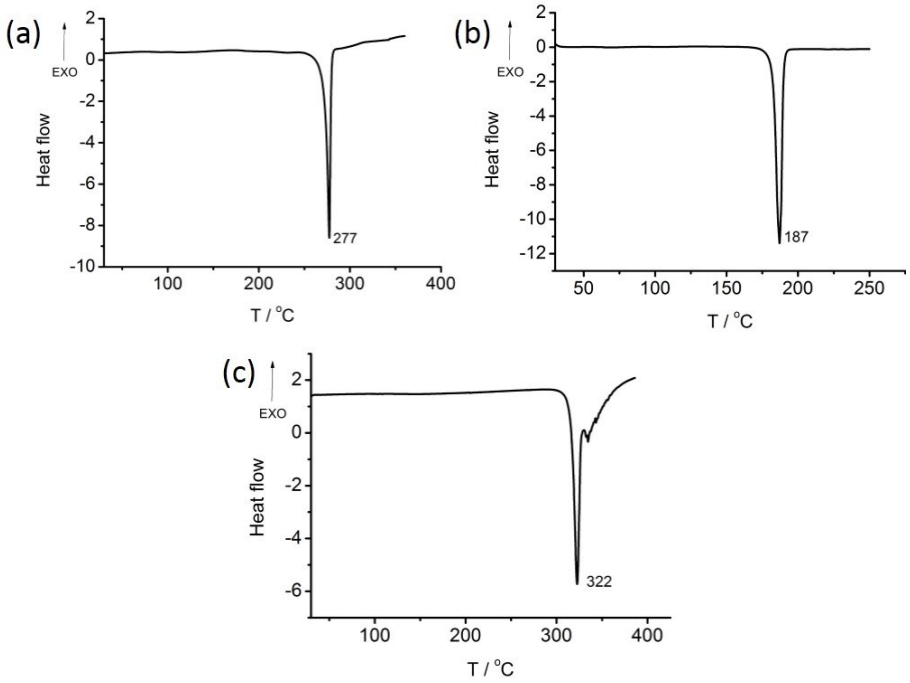

Fig. S21 DSC curves of pristine crystals of **1** (a), **2** (b) and **3** (c).

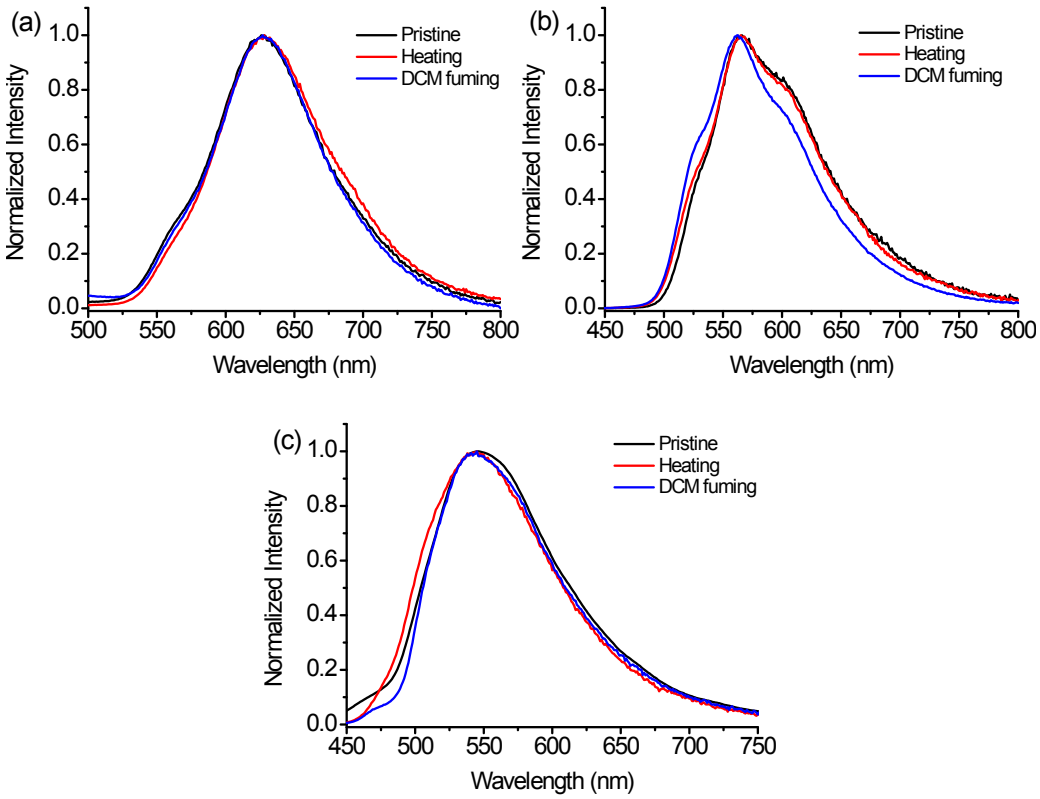

Fig. S22 Normalized emission spectra of **1** (a), **2** (b) and **3** (c) in pristine crystal and treatment with heating and DCM vapour.

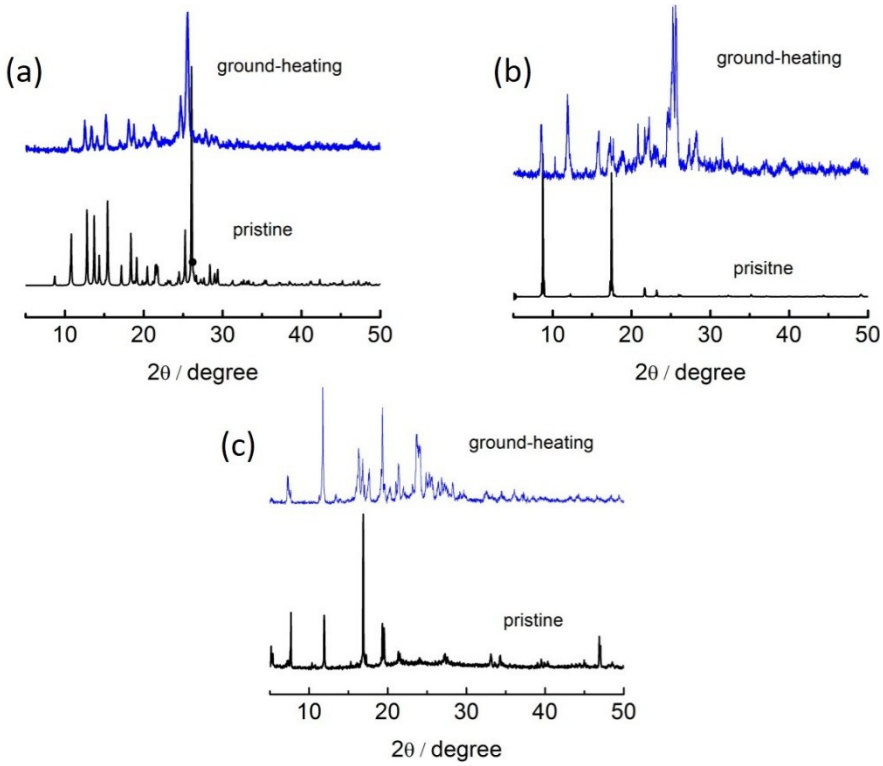

Fig. S23 The XRD patterns of complex **1** (a), **2** (b) and **3** (c) in pristine crystal and after grinding-heating process.

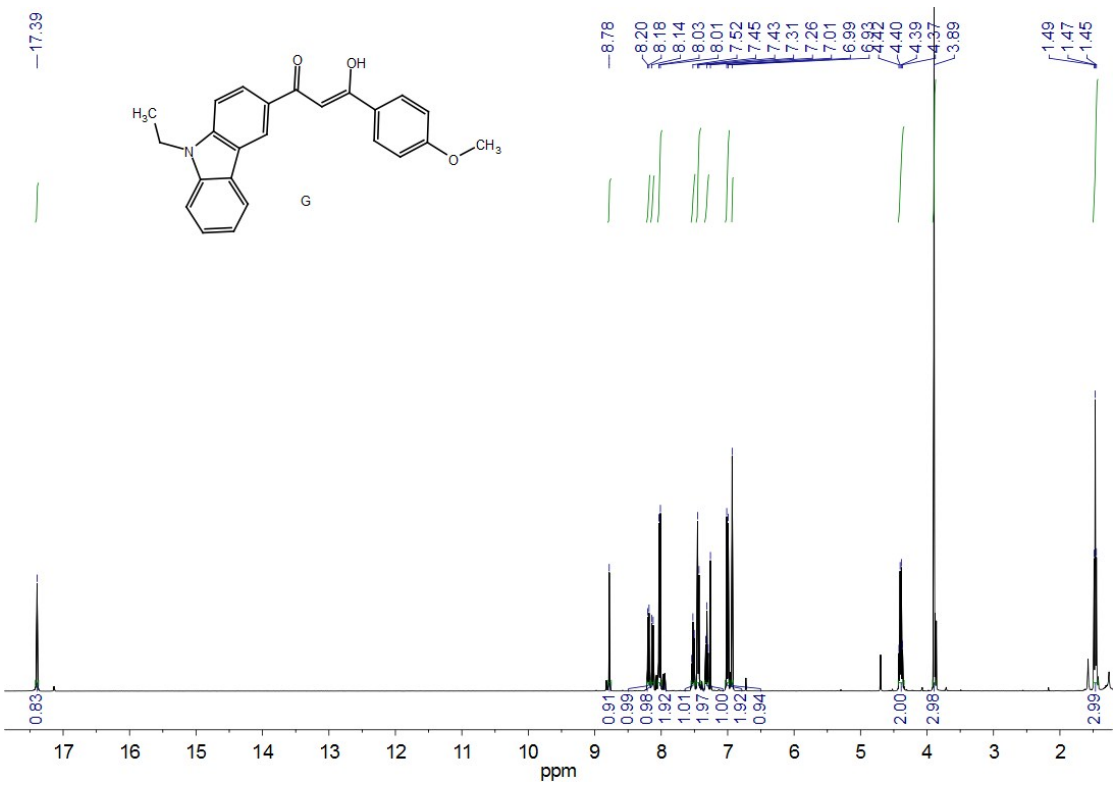

Fig. S24 The ^{1}H NMR spectrum of compound **G** in $CDCl_3$

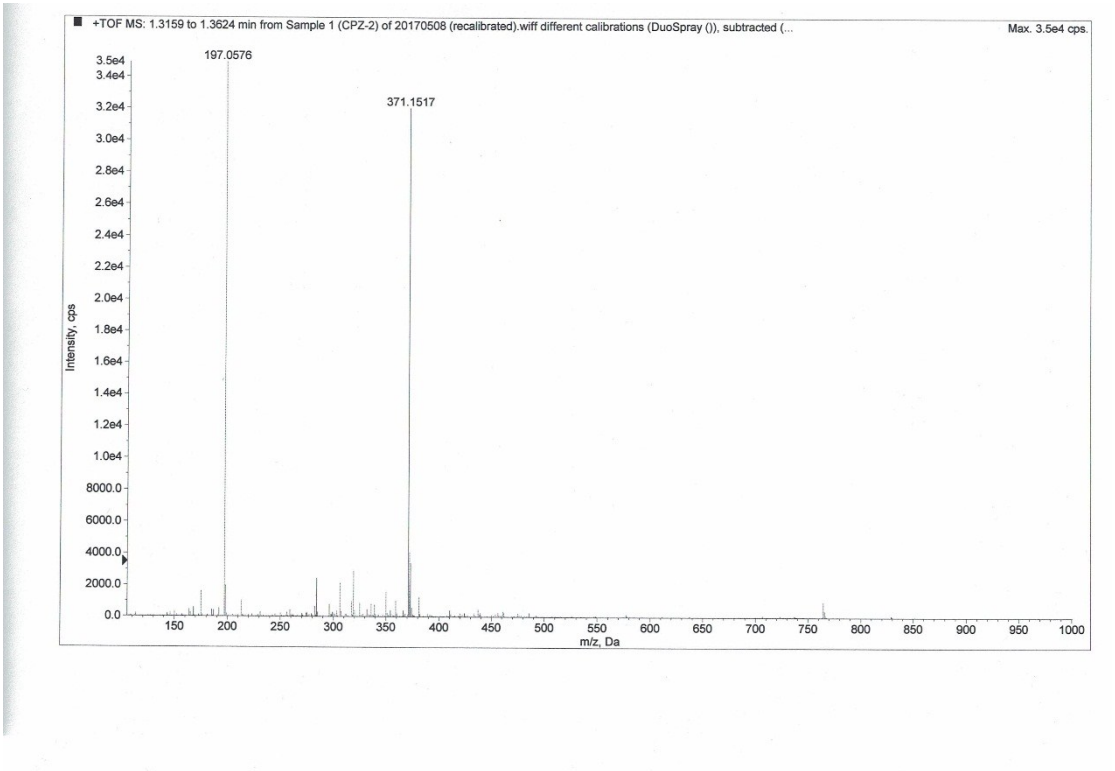

Fig. S25 The HR-MS spectrum of compound **G**.

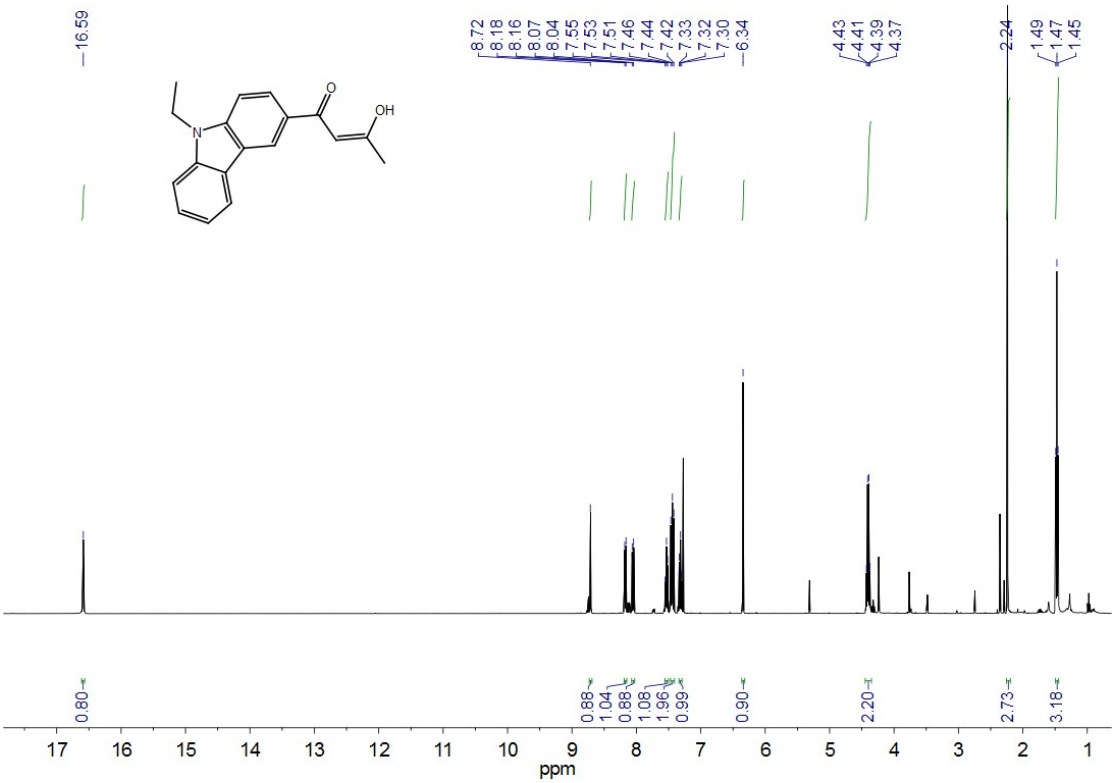

Fig. S26 The ^{1}H NMR spectrum of compound **H** in $CDCl_3$.

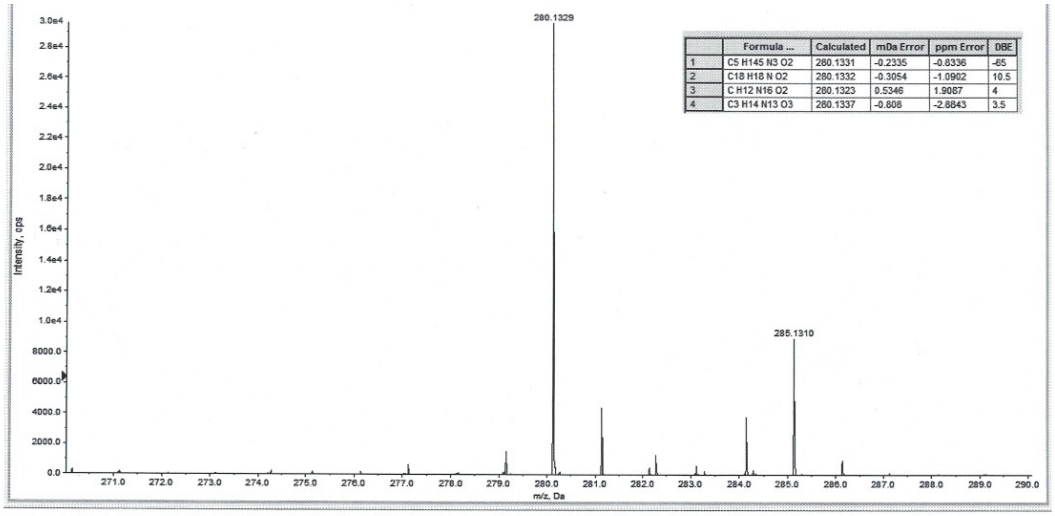

Fig. S27 The HR-MS spectrum of compound **H**.

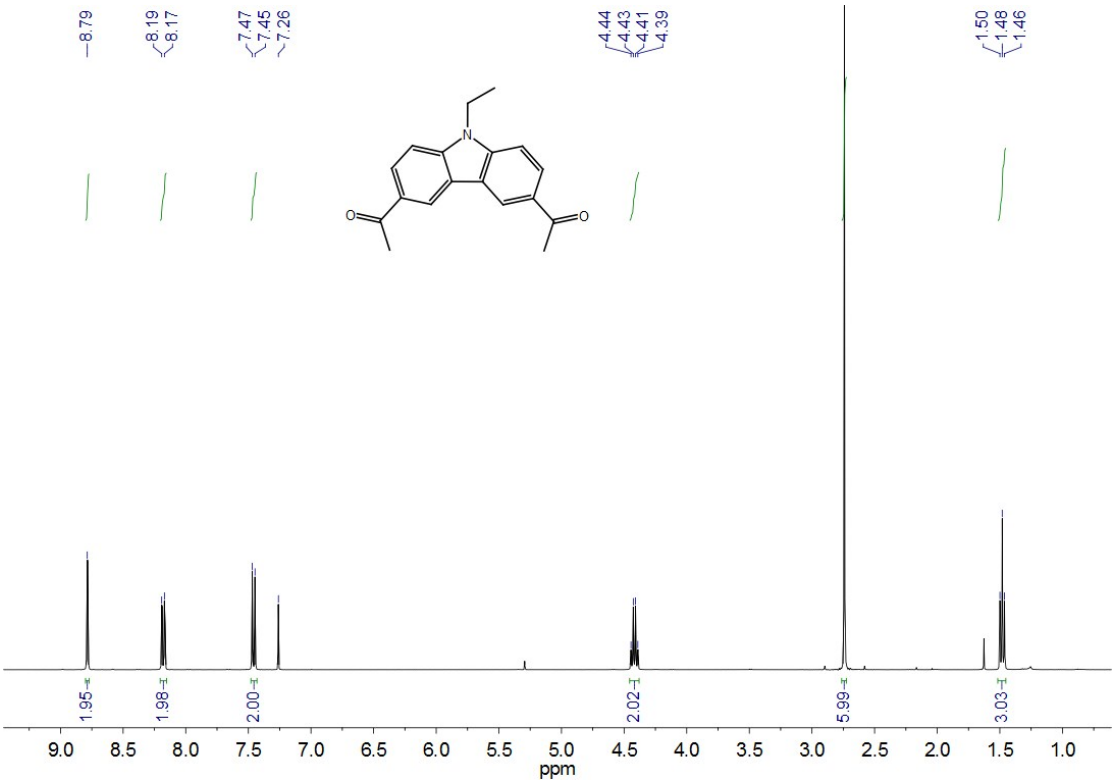

Fig. S28 The ^{1}H NMR spectrum of compound **I** in $CDCl_3$

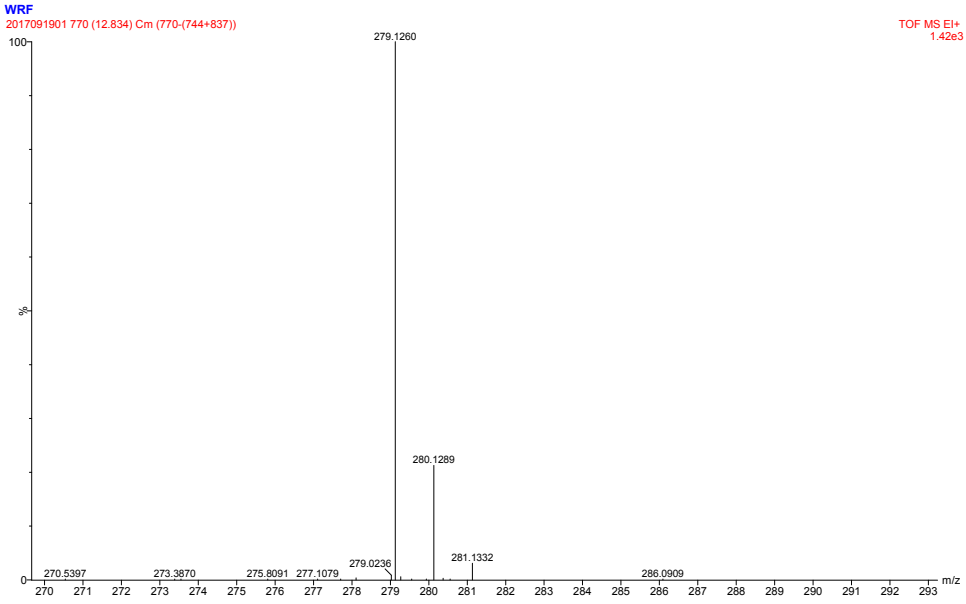

Fig.29 The HR-MS spectrum of compound **I**

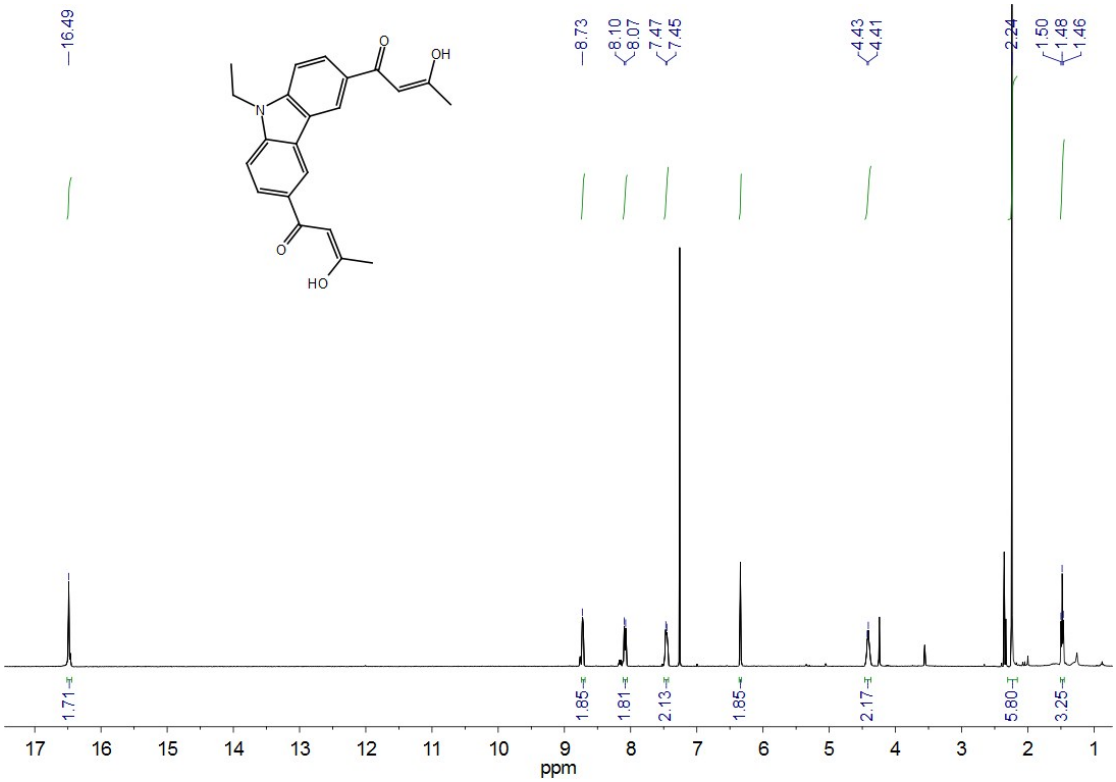

Fig. S30 The ^{1}H NMR spectrum of compound **J** in $CDCl_3$.

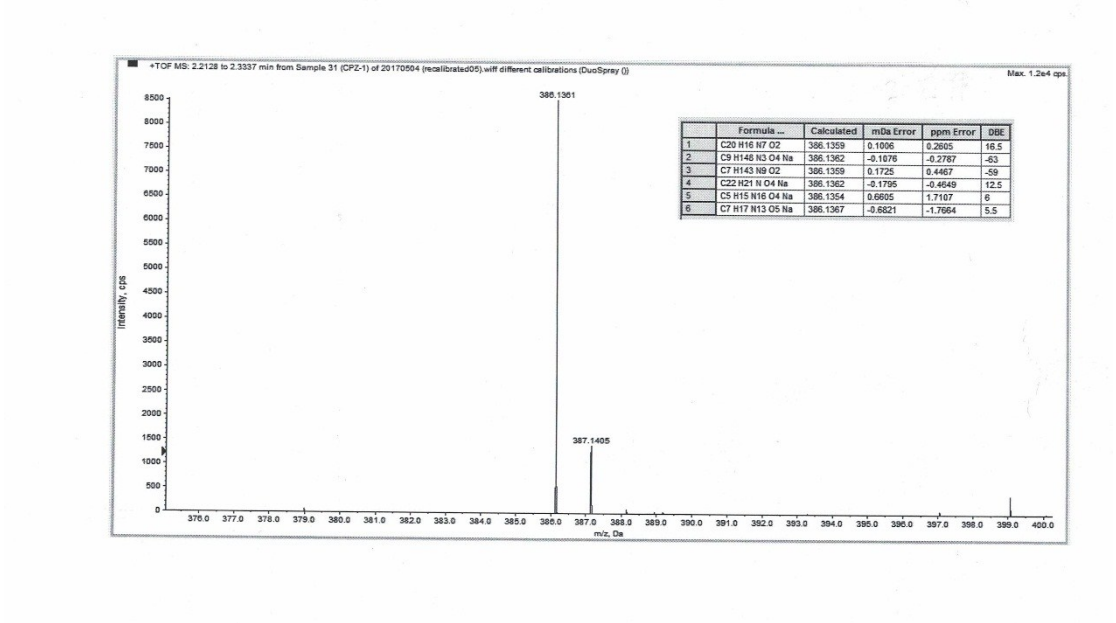

Fig. S31 The HR-MS spectrum of compound **J**.

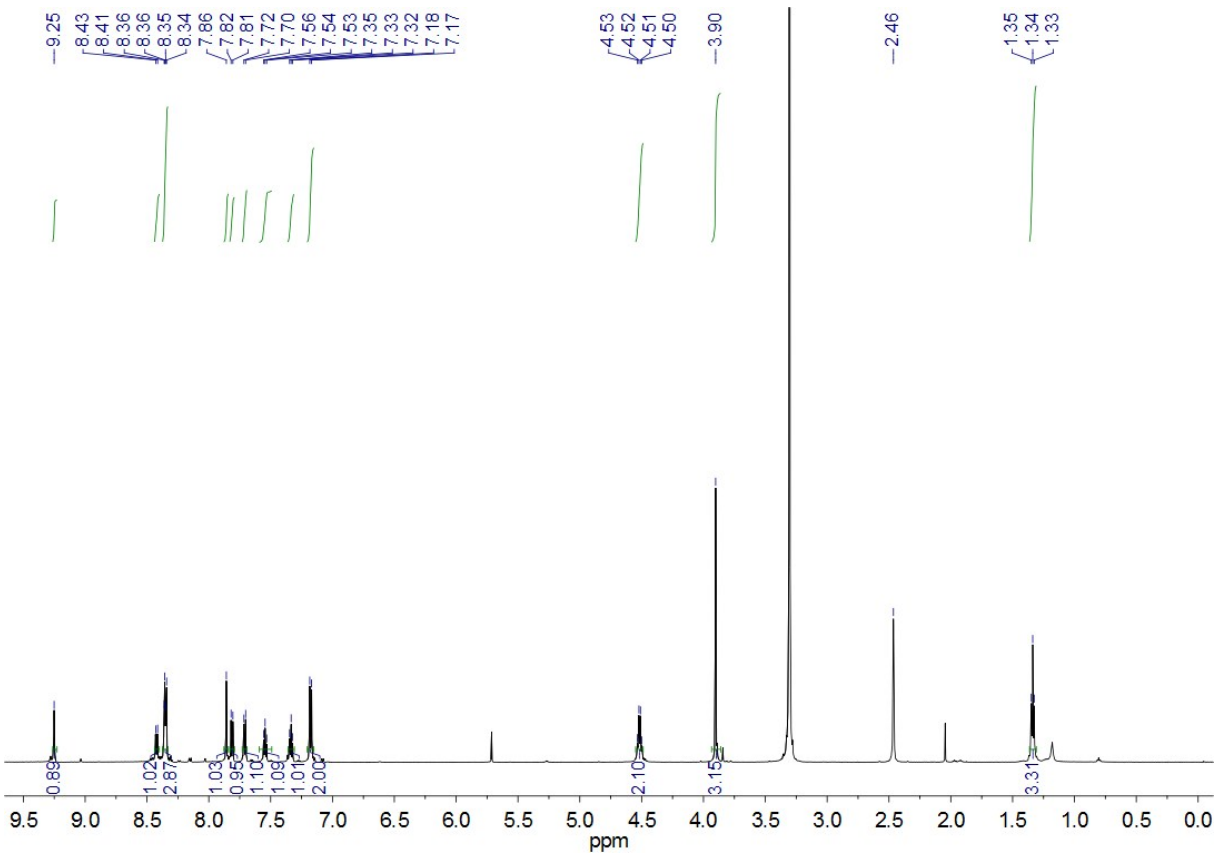

Fig. S32 The ^{1}H NMR spectrum of complex **1** in DMSO-d_6.

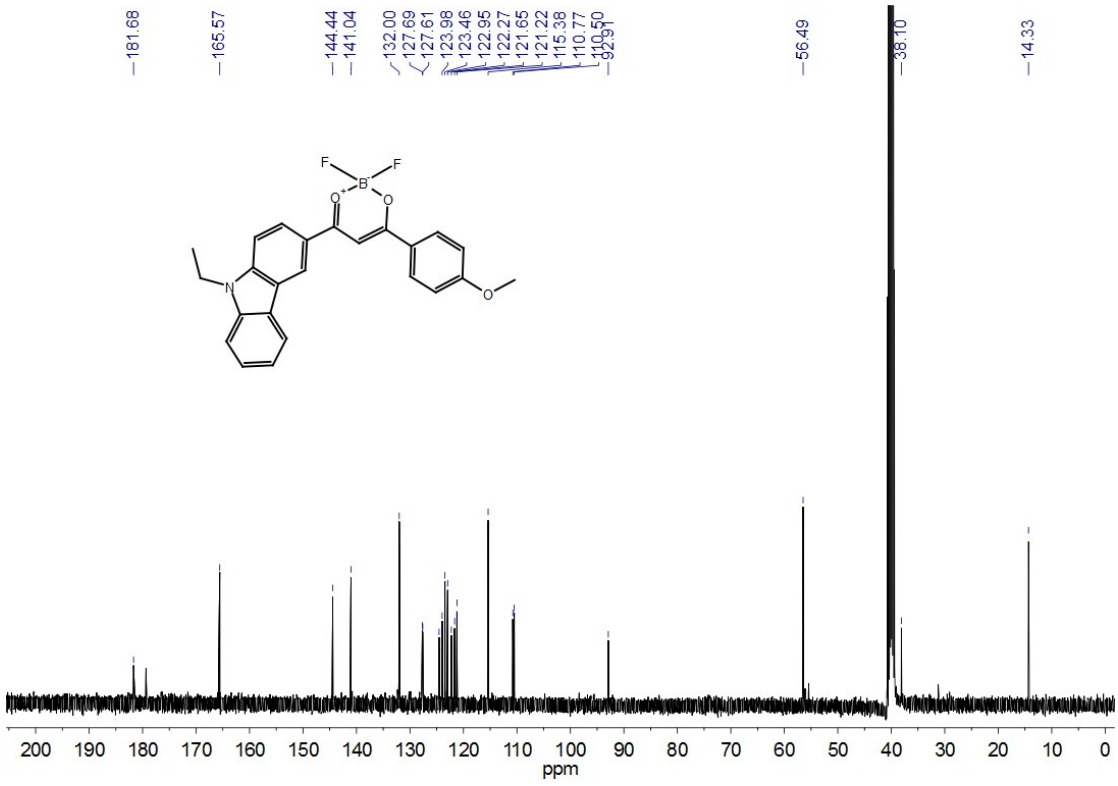

Fig. S33 The ^{13}C NMR spectrum of complex **1** in DMSO-d_6.

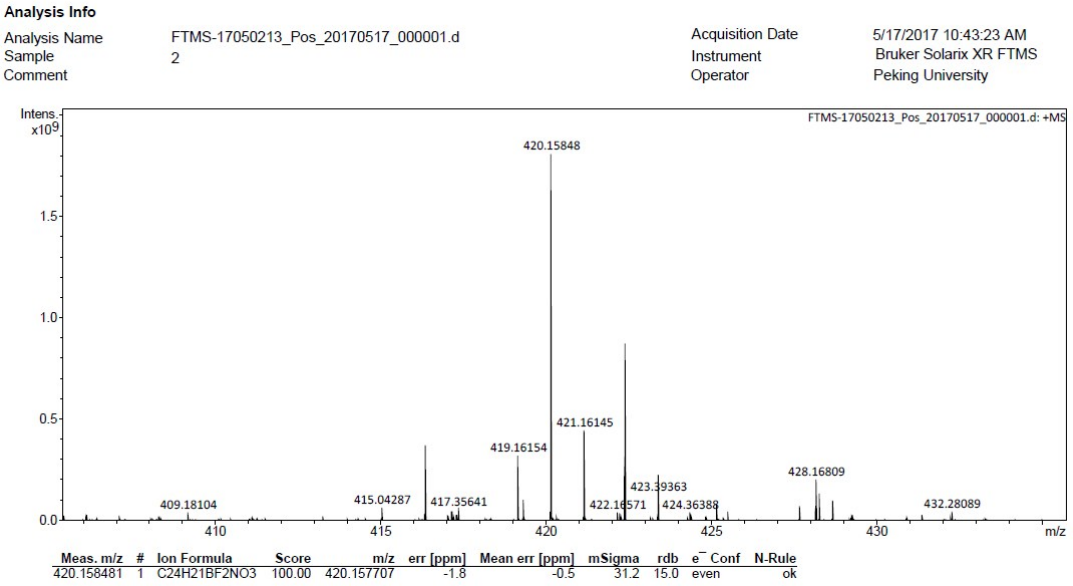

Fig. S34 The HR-MS spectrum of complex **1**.

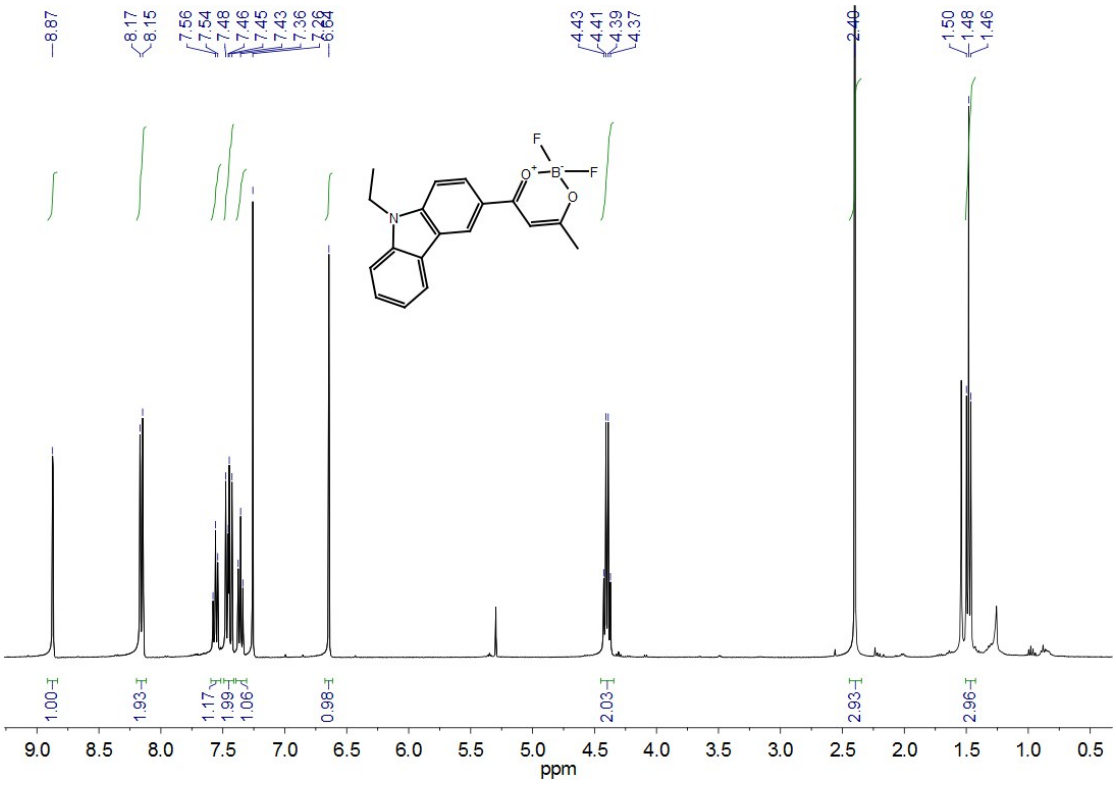

Fig. S35 The ^{1}H NMR spectrum of complex **2** in $CDCl_3$.

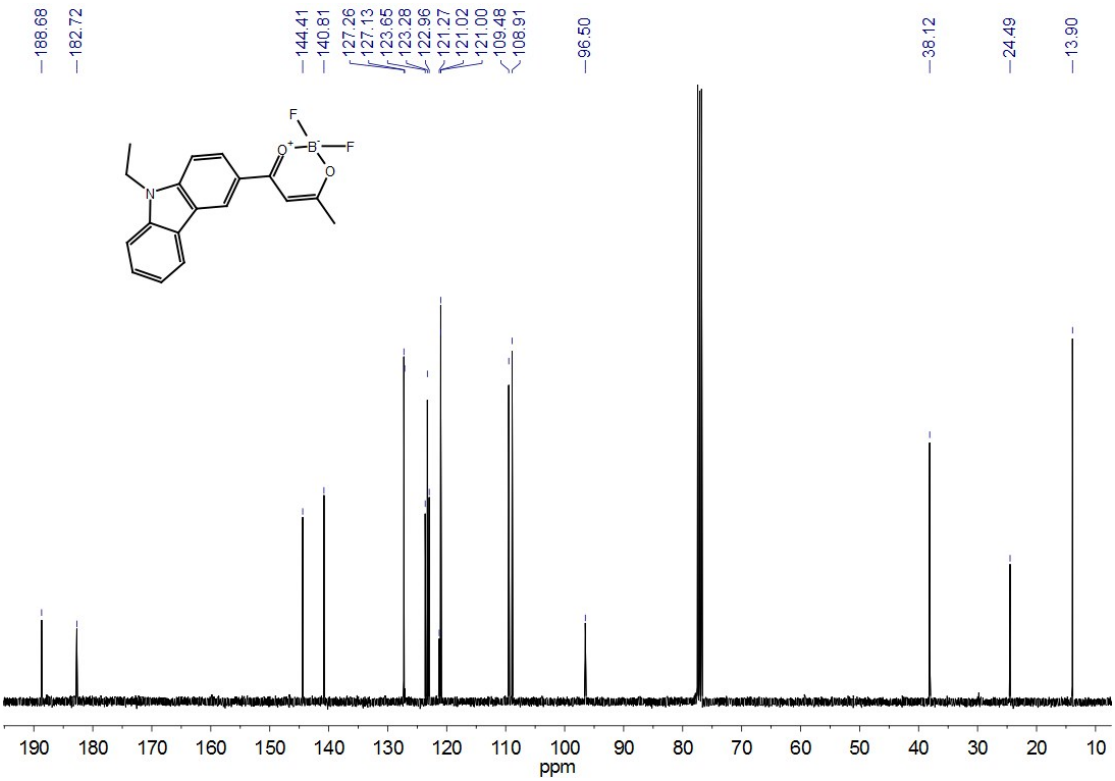

Fig. S36 The ^{13}C NMR spectrum of complex **2** in $CDCl_3$.

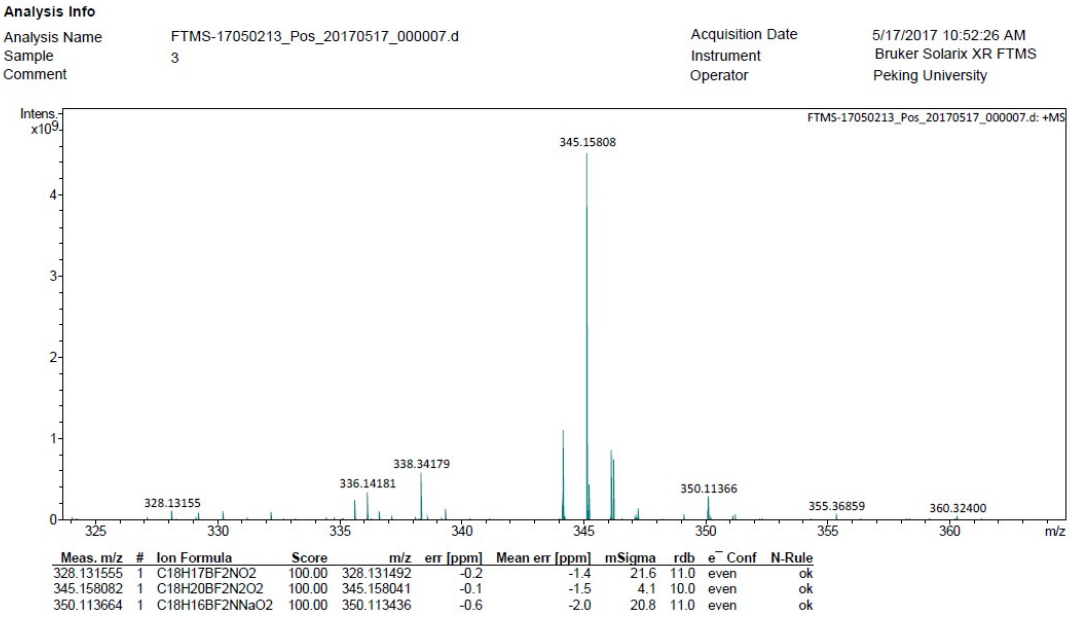

Meas. m/z	#	Ion Formula	Score	m/z	err [ppm]	Mean err [ppm]	mSigma	rdb	e⁻ Conf	N-Rule
328.131555	1	C18H17BF2NO2	100.00	328.131492	-0.2	-1.4	21.6	11.0	even	ok
345.158082	1	C18H20BF2N2O2	100.00	345.158041	-0.1	-1.5	4.1	10.0	even	ok
350.113664	1	C18H16BF2NNaO2	100.00	350.113436	-0.6	-2.0	20.8	11.0	even	ok

Fig. S37 The HR-MS spectrum of complex **2**.

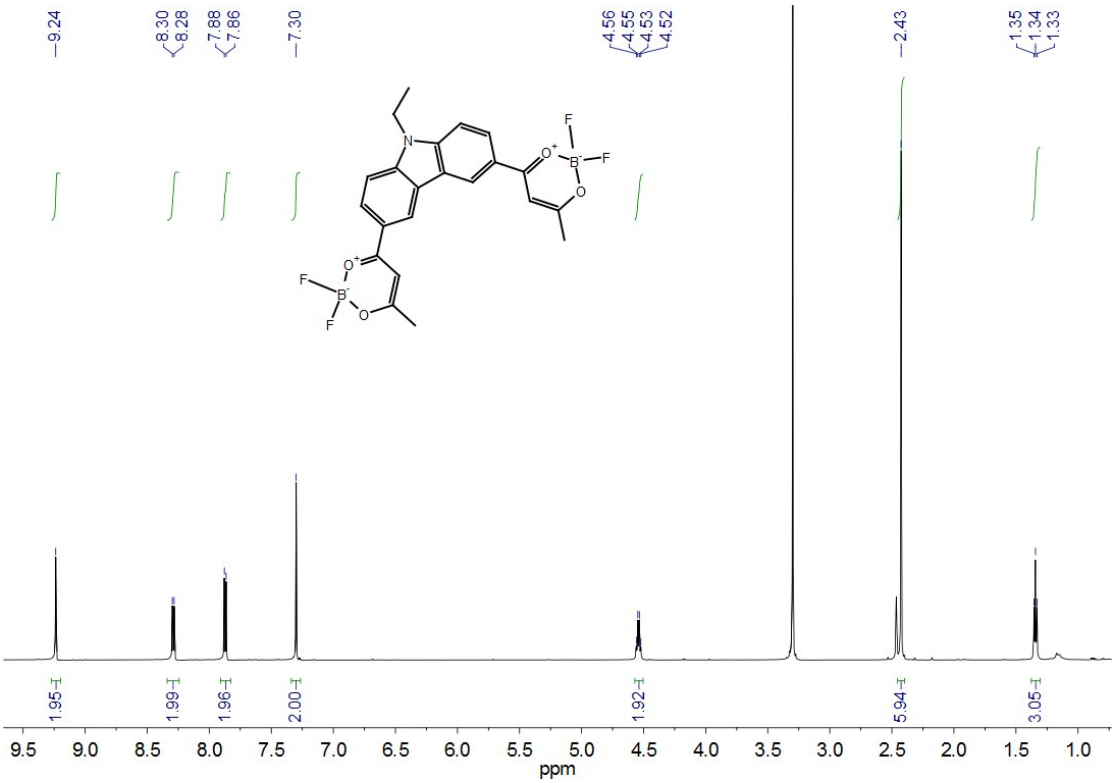

Fig. S38 The ^{1}H NMR spectrum of complex **3** in DMSO-d_6.

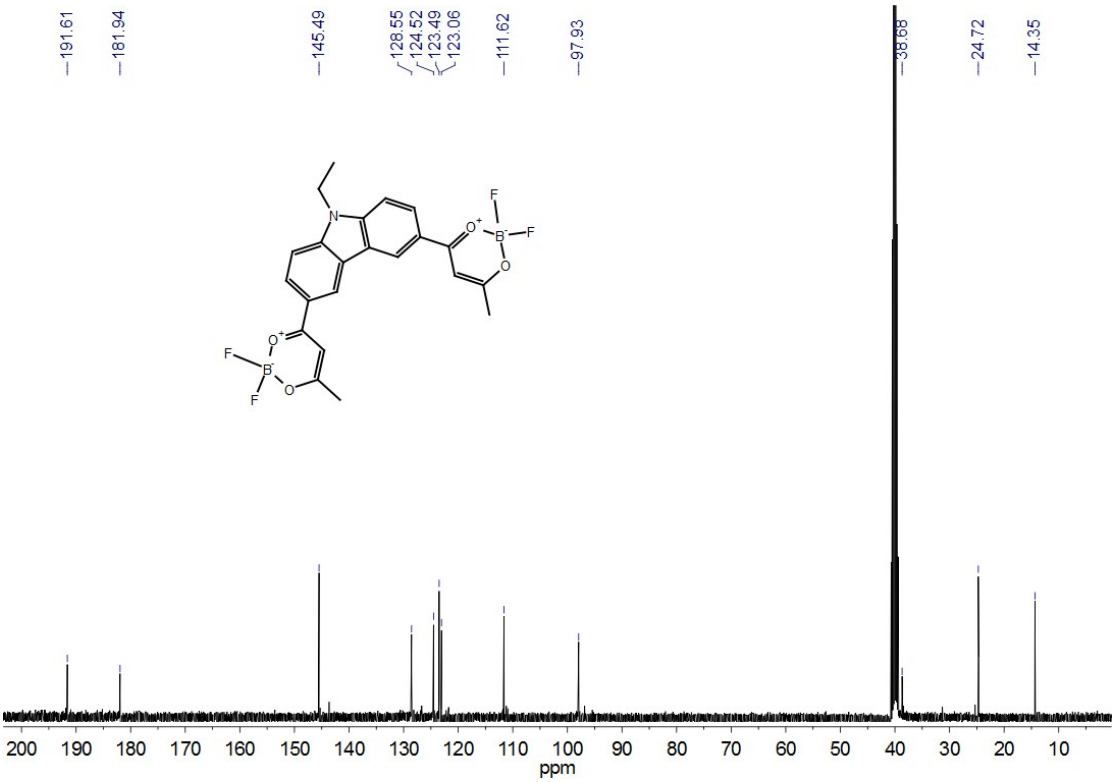

Fig. S39 The ^{13}C NMR spectrum of complex **3** in DMSO-d_6.

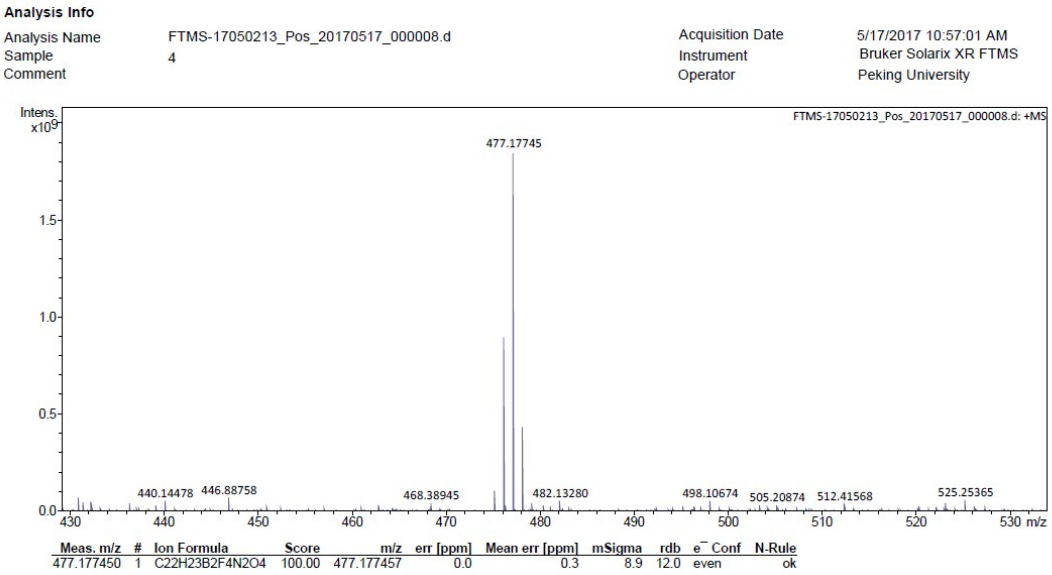

Fig. S40 The HR-MS spectrum of complex **3**.

Reference

S1 P.-Z. Chen, Y.-X. Weng, L.-Y. Niu, Y.-Z. Chen, L.-Z. Wu, C.-H. Tung, Q.-Z. Yang, *Angew. Chem. Int. Ed.*, 2016, **55**, 2759.